



**HAL**  
open science

## **Explorer of Enceladus and Titan (E2 T): Investigating ocean worlds' evolution and habitability in the solar system**

Giuseppe Mitri, Frank Postberg, Jason M. Soderblom, Peter Wurz, Paolo Tortora, Bernd Abel, Jason W. Barnes, Marco Berga, Nathalie Carrasco, Athena Coustenis, et al.

► **To cite this version:**

Giuseppe Mitri, Frank Postberg, Jason M. Soderblom, Peter Wurz, Paolo Tortora, et al.. Explorer of Enceladus and Titan (E2 T): Investigating ocean worlds' evolution and habitability in the solar system. Planetary and Space Science, 2018, 155, pp.73-90. 10.1016/j.pss.2017.11.001 . insu-01636074

**HAL Id: insu-01636074**

**<https://insu.hal.science/insu-01636074v1>**

Submitted on 27 Feb 2018

**HAL** is a multi-disciplinary open access archive for the deposit and dissemination of scientific research documents, whether they are published or not. The documents may come from teaching and research institutions in France or abroad, or from public or private research centers.

L'archive ouverte pluridisciplinaire **HAL**, est destinée au dépôt et à la diffusion de documents scientifiques de niveau recherche, publiés ou non, émanant des établissements d'enseignement et de recherche français ou étrangers, des laboratoires publics ou privés.

# Accepted Manuscript



Explorer of Enceladus and Titan ( $E^2T$ ): Investigating ocean worlds' evolution and habitability in the solar system

Giuseppe Mitri, Frank Postberg, Jason M. Soderblom, Peter Wurz, Paolo Tortora, Bernd Abel, Jason W. Barnes, Marco Berga, Nathalie Carrasco, Athena Coustenis, Jean Pierre Paul de Vera, Andrea D'Ottavio, Francesca Ferri, Alexander G. Hayes, Paul O. Hayne, Jon K. Hillier, Sascha Kempf, Jean-Pierre Lebreton, Ralph D. Lorenz, Andrea Martelli, Roberto Orosei, Anastassios E. Petropoulos, Kim Reh, Juergen Schmidt, Christophe Sotin, Ralf Srama, Gabriel Tobie, Audrey Vorburger, Véronique Vuitton, Andre Wong, Marco Zannoni

PII: S0032-0633(17)30144-7

DOI: [10.1016/j.pss.2017.11.001](https://doi.org/10.1016/j.pss.2017.11.001)

Reference: PSS 4418

To appear in: *Planetary and Space Science*

Received Date: 29 April 2017

Revised Date: 11 September 2017

Accepted Date: 1 November 2017

Please cite this article as: Mitri, G., Postberg, F., Soderblom, J.M., Wurz, P., Tortora, P., Abel, B., Barnes, J.W., Berga, M., Carrasco, N., Coustenis, A., Paul de Vera, J.P., D'Ottavio, A., Ferri, F., Hayes, A.G., Hayne, P.O., Hillier, J.K., Kempf, S., Lebreton, J.-P., Lorenz, R.D., Martelli, A., Orosei, R., Petropoulos, A.E., Reh, K., Schmidt, J., Sotin, C., Srama, R., Tobie, G., Vorburger, A., Vuitton, Vé., Wong, A., Zannoni, M., Explorer of Enceladus and Titan ( $E^2T$ ): Investigating ocean worlds' evolution and habitability in the solar system, *Planetary and Space Science* (2017), doi: 10.1016/j.pss.2017.11.001.

This is a PDF file of an unedited manuscript that has been accepted for publication. As a service to our customers we are providing this early version of the manuscript. The manuscript will undergo copyediting, typesetting, and review of the resulting proof before it is published in its final form. Please note that during the production process errors may be discovered which could affect the content, and all legal disclaimers that apply to the journal pertain.

1 **Explorer of Enceladus and Titan (E<sup>2</sup>T): Investigating Ocean Worlds' Evolution and**  
2 **Habitability in the Solar System**

3

4 Giuseppe Mitri <sup>1</sup>, Frank Postberg <sup>2</sup>, Jason M. Soderblom <sup>3</sup>, Peter Wurz <sup>4</sup>, Paolo Tortora <sup>5</sup>, Bernd Abel  
5 <sup>6</sup>, Jason W. Barnes <sup>7</sup>, Marco Berga <sup>8</sup>, Nathalie Carrasco <sup>9</sup>, Athena Coustenis <sup>10</sup>, Jean Pierre Paul de  
6 Vera <sup>11</sup>, Andrea D'Ottavio <sup>8</sup>, Francesca Ferri <sup>12</sup>, Alexander G. Hayes <sup>13</sup>, Paul O. Hayne <sup>14</sup>, Jon K.  
7 Hillier <sup>15</sup>, Sascha Kempf <sup>16</sup>, Jean-Pierre Lebreton <sup>17</sup>, Ralph D. Lorenz <sup>18</sup>, Andrea Martelli <sup>8</sup>, Roberto  
8 Orosei <sup>19</sup>, Anastassios E. Petropoulos <sup>14</sup>, Kim Reh <sup>14</sup>, Juergen Schmidt <sup>20</sup>, Christophe Sotin <sup>14</sup>, Ralf  
9 Srama <sup>21</sup>, Gabriel Tobie <sup>1</sup>, Audrey Vorburger <sup>4</sup>, Véronique Vuitton <sup>22</sup>, Andre Wong <sup>14</sup>, Marco Zannoni

10 <sup>5</sup>

11 <sup>1</sup> LPG, Université de Nantes, France

12 <sup>2</sup> Klaus-Tschira-Laboratory for Cosmochemistry, University of Heidelberg, Germany

13 <sup>3</sup> Massachusetts Institute of Technology, USA

14 <sup>4</sup> University of Bern, Switzerland

15 <sup>5</sup> University of Bologna, Italy

16 <sup>6</sup> University of Leipzig, Germany

17 <sup>7</sup> University of Idaho, USA

18 <sup>8</sup> Thales Alenia Space, Italy

19 <sup>9</sup> LATMOS, France

20 <sup>10</sup> LESIA, Observ. Paris-Meudon, CNRS, Univ. P. et M. Curie, Univ. Paris-Diderot, France

21 <sup>11</sup> DLR, Germany

22 <sup>12</sup> University of Padova -CISAS, Italy

23 <sup>13</sup> Cornell University, USA

24 <sup>14</sup> Jet Propulsion Laboratory, California Institute of Technology, USA

25 <sup>15</sup> University of Kent, UK

26 <sup>16</sup> University of Colorado, USA

27 <sup>17</sup> LPC2E, France

28 <sup>18</sup> JHU Applied Physics Laboratory, USA

29 <sup>19</sup> INAF, Italy

30 <sup>20</sup> University of Oulu, Finland

31 <sup>21</sup> University of Stuttgart, Germany

32 <sup>22</sup> Univ. Grenoble Alpes, CNRS, IPAG, France

33

34

11 September 2017

35

36

Manuscript submitted to Planetary Space Science

37

38 **Corresponding Author:**

39

40 Giuseppe Mitri

41 Laboratoire de Planetologie et de Geodynamique

42 Université de Nantes

43 2 rue de la Houssinière

44 44322 Nantes, France

45 Giuseppe.Mitri@univ-nantes.fr

46 **Abstract**

47 Titan, with its organically rich and dynamic atmosphere and geology, and Enceladus, with its  
48 active plume, both harbouring global subsurface oceans, are prime environments in which to  
49 investigate the habitability of ocean worlds and the conditions for the emergence of life. We  
50 present a space mission concept, the Explorer of Enceladus and Titan (E<sup>2</sup>T), which is  
51 dedicated to investigating the evolution and habitability of these Saturnian satellites. E<sup>2</sup>T is  
52 proposed as a medium-class mission led by ESA in collaboration with NASA in response to  
53 ESA's M5 Cosmic Vision Call. E<sup>2</sup>T proposes a focused payload that would provide in-situ  
54 composition investigations and high-resolution imaging during multiple flybys of Enceladus  
55 and Titan using a solar-electric powered spacecraft in orbit around Saturn. The E<sup>2</sup>T mission  
56 would provide high-resolution mass spectrometry of the plume currently emanating from  
57 Enceladus' south polar terrain and of Titan's changing upper atmosphere. In addition, high-  
58 resolution infrared (IR) imaging would detail Titan's geomorphology at 50–100 m resolution  
59 and the temperature of the fractures on Enceladus' south polar terrain at meter resolution.  
60 These combined measurements of both Titan and Enceladus would enable the E<sup>2</sup>T mission  
61 scenario to achieve two major scientific goals: 1) Study the origin and evolution of volatile-  
62 rich ocean worlds; and 2) Explore the habitability and potential for life in ocean worlds. E<sup>2</sup>T's  
63 two high-resolution time-of-flight mass spectrometers would enable resolution of the  
64 ambiguities in chemical analysis left by the NASA/ESA/ASI Cassini-Huygens mission  
65 regarding the identification of low-mass organic species, detect high-mass organic species for  
66 the first time, further constrain trace species such as the noble gases, and clarify the evolution  
67 of solid and volatile species. The high-resolution IR camera would reveal the geology of  
68 Titan's surface and the energy dissipated by Enceladus' fractured south polar terrain and  
69 plume in detail unattainable by the Cassini mission.

70 **Keywords:** *Enceladus; Titan; Origin of volatiles; Habitability*

## 71 **1. Introduction**

72 The NASA/ESA/ASI Cassini-Huygens mission has revealed Titan and Enceladus to be two  
73 unique worlds in the Solar System during its thirteen years of observations in the Saturnian  
74 system (July 2004 - September 2017). Titan, with its organically rich and dynamic  
75 atmosphere and geology, and Enceladus, with its active plume system composed of multiple  
76 jets (Waite et al., 2006; Spahn et al., 2006; Porco et al., 2006), both harbouring global  
77 subsurface oceans (Iess et al., 2010, 2012, 2014; see also discussion in Sotin et al., 2010), are  
78 ideal environments in which to investigate the conditions for the emergence of life and the  
79 habitability of ocean worlds as well as the origin and evolution of complex planetary systems.  
80 The prime criteria of habitability include energy sources, liquid water habitats, nutrients and a  
81 liquid transport cycle to move nutrients and waste (McKay et al., 2008, 2016; Lammer et al.,  
82 2009). The best-known candidates in the Solar System for habitability at present meeting  
83 these criteria are the ocean worlds in the outer Solar System, which include: Enceladus, Titan,  
84 Europa, and Ganymede (Lunine, 2016; Nimmo and Pappalardo, 2016). While the Jovian  
85 moons will be thoroughly investigated by the ESA Jupiter Icy moon Explorer (JUICE),  
86 Enceladus and Titan, which provide environments that can be easily sampled from orbit in a  
87 single mission, are currently not targeted by any future exploration. The joint exploration of  
88 these two fascinating objects will allow us to better understand the origin of their organic-rich  
89 environments and will give access to planetary processes that have long been thought unique  
90 to the Earth.

91 Titan is an intriguing world that is similar to the Earth in many ways, with its dense  
92 nitrogen-methane atmosphere and familiar geological features, including dunes, mountains,  
93 seas, lakes and rivers (e.g., Stofan et al., 2007; Lorenz et al., 2006, 2009; Lopes et al., 2007a;  
94 Mitri et al., 2010). Titan undergoes seasonal changes similar to Earth, driven by its orbital  
95 inclination of  $27^\circ$  and Saturn's approximately 30 year orbit. Exploring Titan then offers the

96 possibility to study physical processes analogous to those shaping the Earth's landscape,  
97 where methane takes on water's role of erosion and formation of a distinct geomorphological  
98 surface structure.

99 Enceladus is an enigma; it is a tiny moon (252 km radius) that harbours a subsurface  
100 liquid-water ocean (Iess et al., 2014; McKinnon et al., 2015; Thomas et al., 2016; Čadek et  
101 al., 2016), which jets material into space. The eruption activity of Enceladus offers a unique  
102 possibility to sample fresh material ejected from subsurface liquid water and understand how  
103 exchanges with the interior controls surface activity, as well as to constrain the geochemistry  
104 and astrobiological potential of internal oceans on ocean worlds (e.g., Porco et al., 2006).  
105 Since the 1997 launch of the Cassini-Huygens mission, there has been great technological  
106 advancement in instrumentation that would enable answering key questions that still remain  
107 about the Saturnian ocean worlds.

108 The scientific appeal of Titan and Enceladus has stimulated many previous mission studies  
109 (e.g. see reviews by Lorenz, 2000; 2009), which have articulated detailed scientific objectives  
110 for post-Cassini scientific exploration (e.g. Mitri et al., 2014a; Tobie et al., 2014). At Titan, in  
111 particular, the diversity of scientific disciplines (Dougherty et al., 2009) has prompted the  
112 study of a variety of observing platforms from orbiters ("Titan Explorer", Leary et al., 2007;  
113 Mitri et al., 2014a), landers for the seas ("Titan-Saturn System Mission – TSSM", Strange et  
114 al., 2009; "Titan Mare Explorer - TiME", Stofan et al., 2013, Mitri et al., 2014a), landers for  
115 land (Titan Explorer), fixed-wing aircraft ("AVIATR", Barnes et al., 2012), to balloons (Titan  
116 Explorer, TSSM and others). Additionally, Enceladus' plume has attracted designs of  
117 spacecraft to sample it: "Titan and Enceladus Mission TANDEM" (Coustenis et al., 2009),  
118 "Journey to Enceladus and Titan – JET" and "Enceladus Life Finder – ELF" (Reh et al.,  
119 2016).

120 We present a space mission concept, the Explorer of Enceladus and Titan (E<sup>2</sup>T), which is  
121 dedicated to investigating the evolution and habitability of these Saturnian satellites and is  
122 proposed as a medium-class mission led by ESA in collaboration with NASA in response to  
123 ESA's M5 Cosmic Vision Call. In Section 2 we present the science case for the future  
124 exploration of Enceladus and Titan as proposed by the E<sup>2</sup>T mission, and Section 3 the science  
125 goals for the E<sup>2</sup>T mission. In Sections 4 and 5 we discuss the proposed payload and mission  
126 and spacecraft configuration necessary to achieve E<sup>2</sup>T mission goals.

127

## 128 **2. Science Case for the Exploration of Enceladus and Titan**

129 Titan, Saturn's largest satellite, is unique in the Solar System with its dense, extensive  
130 atmosphere composed primarily of nitrogen (97%) and methane (1.4%) (e.g., Bézard, 2014),  
131 and a long list of organic compounds resulting from multifaceted photochemistry that occurs  
132 in the upper atmosphere down to the surface (e.g., Israël et al., 2005; Waite et al., 2007;  
133 Gudipati et al., 2013; Bézard, 2014). As methane is close to its triple point on Titan, it gives  
134 rise to a methane cycle analogous to the terrestrial hydrological cycle, characterized by cloud  
135 activity, precipitation, river networks, lakes and seas covering a large fraction of the northern  
136 terrain (Figure 1) (e.g., Tomasko et al., 2005; Stofan et al., 2007; Mitri et al., 2007; Lopes et  
137 al., 2007a; Hayes et al., 2008).

138

### FIGURE 1

139 With an environment that changes on a 29.5 year cycle, it is crucial to study Titan during  
140 an entire orbital period. Cassini has investigated Titan over only two seasons: from Northern  
141 winter solstice to summer solstice. While ground-based observations, have observed Titan in  
142 other seasons, these data are not sufficient to address many of the outstanding questions.  
143 Current measurements with Cassini/CIRS show that the chemical content of Titan's  
144 atmosphere has significant seasonal and latitudinal variability (Coustenis et al., 2013; 2016);



145 future extended exploration of Titan is necessary to get a full picture of the variations within  
146 this complex environment.

147 Titan is the only known planetary body, other than the Earth, with long-standing liquid on  
148 its surface, albeit hydrocarbons instead of water; these lakes and seas are likely fed by a  
149 combination of precipitation, surface runoff and subsurface alkanofers (hydrocarbon  
150 equivalent of aquifers) in the icy crust (Hayes et al., 2008). The presence of radiogenic noble  
151 gases in the atmosphere indicates some communication between the surface and the  
152 subsurface and is suggestive of water-rock interactions and methane outgassing processes  
153 (Tobie et al., 2012), possibly associated with cryovolcanic activity or other exchange  
154 processes (Lopes et al., 2007b, 2016; Solomonidou et al., 2014, 2016). The detection of a  
155 salty ocean at an estimated 50-80 km depth (Iess et al., 2012; Beghin et al., 2012; Mitri et al.,  
156 2014b) and the possible communication between this ocean and the organic-rich surface hint  
157 at exciting astrobiological possibilities. While Cassini has provided tantalizing views of the  
158 surface with its lakes and seas, dunes, equatorial mountains, impact craters and possible  
159 cryovolcanos, the low spatial, spectral, and mass resolution of the Cassini scientific  
160 instruments make it difficult to identify morphological features, to quantify geological  
161 processes and relationships between different geological units and to monitor changes due to  
162 geologic or atmospheric activity. Constraining the level of geological activity on Titan is  
163 crucial to understanding its evolution and determining if this ocean world could support  
164 abiotic/prebiotic activity.

165 Both Titan and Enceladus possess several, if not all, of the key ingredients necessary for  
166 life: an energy source, liquid habitats, nutrients (organic compounds) and a liquid transport  
167 cycle to move nutrients and waste (McKay et al., 2008, 2016). While sunlight is a minimal  
168 source of energy for solid bodies in the outer Solar System, interior heat sources derived from  
169 a rocky core or tidal forces produced by neighbouring satellites and planet can be quite

170 significant. Most recently, the Cassini INMS has identified molecular hydrogen at the level of  
171 0.4–1.4% in Enceladus' plume (Waite et al., 2017) providing further evidence of water-rock  
172 interactions. This suggests that methane formation from CO<sub>2</sub> in Enceladus' subsurface ocean  
173 could occur in a similar fashion as it occurs on Earth, where extremophile microbes in  
174 hydrothermal sea vents produce methane as a metabolic by-product (McKay et al., 2008).  
175 Another compelling discovery is the complex large nitrogen-bearing organic molecules in  
176 Titan's upper atmosphere by Cassini (Waite et al., 2007; Coates et al., 2007). The low  
177 resolution of the in-situ mass spectrometers on Cassini, however, precludes the determination  
178 of the chemical composition of this complex organic matter. In situ exploration with more  
179 advanced instruments is required to investigate the prebiotic potential of Titan.

180 The discovery in 2005 of a plume emanating from multiple jets in Enceladus' south polar  
181 terrain is one of the major highlights of the Cassini–Huygens mission (Figure 2) (Dougherty  
182 et al., 2006; Porco et al., 2006; Spahn et al., 2006). Despite its small size (10 times smaller  
183 than Titan), Enceladus is the most geologically active moon of the Saturnian system.  
184 Although geyser-like plumes have been observed on Triton (Soderblom et al., 1990) and more  
185 recently transient water vapour activity around Europa has been reported (Roth et al., 2014;  
186 Sparks et al., 2016, 2017), Enceladus is the only satellite for which this activity is known to  
187 be endogenic in nature. The jets, of which approximately one hundred have been identified  
188 (Porco et al., 2014) form a huge plume of vapour and ice grains above Enceladus' south polar  
189 terrain and are associated with elevated heat flow along tectonic ridges, called 'tiger stripes'.  
190 Enceladus' endogenic activity and gravity measurements indicate that it is a differentiated  
191 body, providing clues to its formation and evolution (Iess et al., 2014). Sampling of the plume  
192 by Cassini's instruments revealed the presence of water vapour, ice grains rich in sodium and  
193 potassium salts (Postberg et al., 2011). Organic materials were observed, both in the gas  
194 (Waite et al., 2009) and in the ice grains (Postberg et al., 2008, 2015), and molecular

195 hydrogen (Waite et al., 2017). The jet sources are connected to a subsurface salt-water  
196 reservoir that is likely alkaline in nature and undergoing hydrothermal water-rock interactions  
197 (Porco et al., 2006, 2014; Waite et al., 2006, 2009, 2017; Postberg et al., 2009, 2011; Hsu et  
198 al., 2011, 2014; Glein et al., 2015). The putative exothermic water-rock interactions on  
199 Enceladus could be further constrained by quantifying He and constraining the amount of H<sub>2</sub>  
200 in the plume. Gravity, topography and libration measurements demonstrate the presence of a  
201 global subsurface ocean (Iess et al., 2014; McKinnon et al., 2015; Thomas et al., 2016; Čadek  
202 et al., 2016; Beuthe et al., 2016). The co-existence of organic compounds, salts, liquid water  
203 and energy sources on this small moon appear to provide all of the necessary ingredients for  
204 the emergence of life by chemoautotrophic pathways (McKay et al., 2008) – a generally held  
205 model for the origin of life on Earth in deep sea vents.

## 206 FIGURE 2

207 Titan and Enceladus offer an opportunity to study analogous prebiotic processes that may  
208 have led to the emergence of life on Earth. Retracing the processes that allowed the  
209 emergence of life on Earth around 4 Ga is a difficult challenge since most traces of the  
210 environmental conditions at that time have been erased. It is, therefore, crucial for  
211 astrobiologists to find extraterrestrial planetary bodies with similarities to our planet,  
212 providing a way to study some of the processes that occurred on the primitive Earth, when  
213 prebiotic chemistry was active. The eruption activity of Enceladus offers a possibility to  
214 sample fresh material emerging from subsurface liquid water and to understand how exchange  
215 processes with the interior control surface activity. It provides us with an opportunity to study  
216 phenomena in-situ that has been important in the past on Earth and throughout the outer Solar  
217 System.

218

219

### 220 3. Scientific Objectives and Investigations

221 The proposed E<sup>2</sup>T mission has two major goals and several science objectives that would be  
222 pursued through Enceladus and Titan investigations. The first scientific goal of the E<sup>2</sup>T  
223 mission on Enceladus would focus on the origin and evolution of volatile compounds in the  
224 plume vapour and icy grains. On Titan the first scientific goal includes two objectives; the  
225 first would focus on determining the history and extent of volatile exchange on Titan and the  
226 second objective would aim to understand how Titan's surface processes evolved. The second  
227 scientific goal on Enceladus would examine the nature of hydrothermal activity and search for  
228 evidence of abiotic/prebiotic processes. On Titan, the second scientific goal would aim to  
229 discern to what level of complexity abiotic/prebiotic chemistry has evolved. The scientific  
230 objectives and investigations of E<sup>2</sup>T are discussed in detail in the Sections 3.1 and 3.2; Table  
231 1 details the scientific objectives, the scientific questions, and the measurements requirements  
232 (payload, instrument parameters) to address the scientific goals of the E<sup>2</sup>T mission.

233 Enceladus and Titan' investigations would be conducted using the E<sup>2</sup>T mission model  
234 payload, which consists of three instruments: two time-of-flight mass spectrometers, the Ion  
235 and Neutral Gas Mass Spectrometer (INMS) and the Enceladus Icy Jet Analyzer (ENIJA)  
236 dust instrument; and a high-resolution infrared (IR) camera, the Titan Imaging and Geology,  
237 Enceladus Reconnaissance (TIGER). The scientific payload will be described in Section 4.

238 TABLE 1

### 240 3.1 Origin and Evolution of Volatile-Rich Ocean Worlds in the Saturn System

#### 241 3.1.1 Chemical Constraints on the Origin and Evolution of Titan and Enceladus

242 The origin and evolution of Titan's methane still needs to be constrained. It is a key open  
243 question whether Titan's methane is primordial likely due to water-rock interactions in  
244 Titan's interior during its accretionary phase (Atreya et al., 2006) or else is delivered to Titan  
245 during its formation processes (Mousis et al., 2009) or by cometary impacts (Zahnle et al.,  
246 1992; Griffith and Zahnle, 1995). On Titan, the Huygens probe detected a small argon  
247 abundance ( $^{36}\text{Ar}$ ) and a tentative amount of neon ( $^{22}\text{Ne}$ ) in its atmosphere (Niemann et al.,  
248 2005, 2010), but was unable to detect the corresponding abundance of xenon and krypton.  
249 The presence of  $^{22}\text{Ne}$  ( $^{36}\text{Ar}/^{22}\text{Ne}\sim 1$ ) was unexpected, as neon is not expected to be present in  
250 any significant amounts in protosolar ices (Niemann et al., 2005, 2010), and may indicate  
251 water-rock interactions and outgassing processes (Tobie et al., 2012). The non-detection of  
252 xenon and krypton supports the idea that Titan's methane was generated by serpentinization  
253 of primordial carbon monoxide and carbon dioxide delivered by volatile depleted  
254 planetesimals originating from within Saturn's subnebula (e.g., Atreya et al., 2006). To  
255 support a primordial methane source, xenon and krypton both would have to be sequestered  
256 from the atmosphere. While xenon is soluble in liquid hydrocarbon (solubility of  $10^{-3}$  at 95 K)  
257 and could potentially be sequestered into liquid reservoirs, argon and krypton cannot be  
258 sequestered as soluble materials (Cordier et al., 2010). Therefore, the absence of measureable  
259 atmospheric krypton requires either sequestration into non-liquid surface deposits, such as  
260 clathrates (Mousis et al., 2011), or depletion in the noble gas concentration of the  
261 planetesimals (Owen and Niemann, 2009). Unlike Cassini INMS, the E<sup>2</sup>T INMS has the mass  
262 range and the sensitivity to accurately measure xenon. E<sup>2</sup>T would measure the abundance of  
263 noble gases in the upper atmosphere of Titan to discriminate between crustal carbon  
264 sequestration and carbon delivery via depleted planetesimals.

265 The longevity of methane in Titan's atmosphere is still a mystery. The value of  $^{12}\text{C}/^{13}\text{C}$  in  
266 Titan's atmosphere has been used to conclude that methane outgassed  $\sim 10^7$  years ago (Yung

267 et al., 1984), and is being lost via photolysis and atmospheric escape (Yelle et al., 2008). It is  
268 an open question whether the current methane rich atmosphere is a unique event, in a steady  
269 state where methane destruction and replenishment are in balance (Jennings et al., 2009), or is  
270 a transient event and is in a non-steady state where methane is being actively depleted or  
271 replenished. Indeed, the possibility that Titan did not always possess a methane rich  
272 atmosphere seems to be supported by the fact that the amount of ethane on Titan's surface  
273 should be larger than the present inventory; though Wilson and Atreya (2009) contend that  
274 missing surface deposits may simply be reburied into Titan's crust and Mousis and Schmitt  
275 (2008) have shown that it is possible for liquid ethane to react with a water-ice and methane-  
276 clathrate crust to create ethane clathrates and release methane. Nixon et al. (2012), however,  
277 favours a model in which methane is not being replenished and suggest atmospheric methane  
278 duration is likely between 300 and 600 Ma given that Hörst et al. (2008) demonstrated that  
279 300 Ma is necessary to create Titan's current CO inventory and recent surface age estimates  
280 based on cratering (Neish and Lorenz, 2012). Mandt et al. (2012) suggests that methane's  
281 presence in the atmosphere, assumed here to be due to outgassing, has an upper limit of 470  
282 Ma or else up to 940 Ma if the presumed methane outgassing rate was large enough to  
283 overcome  $^{12}\text{C}/^{13}\text{C}$  isotope fractionation resulting from photochemistry and escape. Both the  
284 results of Mandt et al. (2012) and Nixon et al. (2012) fall into the timeline suggested by  
285 interior models (Tobie et al., 2006) which suggests that the methane atmosphere is the result  
286 of an outgassing episode that occurred between 350 and 1350 Ma. On Titan, both simple  
287 (methane, ethane and propane) and complex hydrocarbons precipitate out of the atmosphere  
288 onto the surface. Measuring the isotopic ratios ( $^{14}\text{N}/^{15}\text{N}$ ;  $^{12}\text{C}/^{13}\text{C}$ ; D/H;  $^{16}\text{O}/^{18}\text{O}$ ;  $^{17}\text{O}/^{16}\text{O}$ ) and  
289 abundances of the simple alkanes (e.g., methane, ethane and propane) would constrain the  
290 formation and evolution of the methane cycle on Titan. Further measurements of radiogenic  
291 noble gases such as  $^{40}\text{Ar}$  and  $^{22}\text{Ne}$ , which are typically markers of volatile elements from

292 Titan's interior can constrain outgassing episodes. Detection of  $^{40}\text{Ar}$  and tentatively  $^{22}\text{Ne}$  in  
293 the atmosphere has provided circumstantial evidence of water-rock interactions and methane  
294 outgassing from the interior (Niemann et al., 2010; Tobie et al., 2012). Recent measurements  
295 by ground-based observatories including measurements of CO and its carbon and oxygen  
296 isotopologues accompanied by the first detection of  $^{17}\text{O}$  in Titan and indeed in the outer Solar  
297 System by Atacama Large Millimeter/submillimeter Array (ALMA) can be followed up on in  
298 more detail by in-situ spectroscopic measurements (Serigano et al., 2016). E<sup>2</sup>T would  
299 measure the composition and isotopic ratios of Titan's upper atmosphere to determine the age  
300 of methane in the atmosphere and characterize outgassing history.

301 On Enceladus, Cassini measurements by INMS (Waite et al., 2006, 2009, 2017) and UVIS  
302 (Hansen et al., 2006, 2008) showed that plume gas consists primarily of water vapour with a  
303 few percent other volatiles. In addition to  $\text{H}_2\text{O}$ , as the dominant species, INMS was able to  
304 identify  $\text{CO}_2$  (0.3-0.8%),  $\text{CH}_4$  (0.1-0.3%),  $\text{NH}_3$  (0.4-1.3%) and  $\text{H}_2$  (0.4-1.4%), in the vapour  
305 plume as well as an unidentified species with a mass-to-charge ( $m/z$ ) ratio of 28, which is  
306 thought to be either  $\text{N}_2$  or  $\text{C}_2\text{H}_4$ , a combination of these compounds, or CO. The low mass  
307 resolution of Cassini INMS is insufficient to separate these species, and the UVIS  
308 measurements can only provide upper limits on  $\text{N}_2$  and CO abundance. Determining the  
309 abundance ratio between these different species is, however, essential to constrain the origin  
310 of volatiles on Enceladus and to assess if they were internally reprocessed. A high  $\text{CO}/\text{N}_2$   
311 ratio, for instance, would suggest a cometary-like source with only a moderate modification  
312 of the volatile inventory, whereas a low  $\text{CO}/\text{N}_2$  ratio would indicate significant internal  
313 reprocessing.

314 In addition to these main volatile species, the possible presence of trace quantities of  $\text{C}_2\text{H}_2$ ,  
315  $\text{C}_3\text{H}_8$ , methanol, formaldehyde and hydrogen sulphide has been detected within the INMS  
316 data recorded during some Cassini flybys (Waite et al., 2009). Organic species above the

317 INMS mass range of 99 u are also present but could not be further constrained (Waite et al.,  
318 2009). The identification and the quantification of the abundances of these trace species  
319 remains very uncertain due to the limitations of the mass spectrometer onboard Cassini.

320 Except for the measurement of D/H in H<sub>2</sub>O on Enceladus (which has large uncertainty,  
321 Waite et al., 2009), no information is yet available for the isotopic ratios in Enceladus' plume  
322 gas. The E<sup>2</sup>T mission would determine the isotopic ratios (D/H, <sup>12</sup>C/<sup>13</sup>C, <sup>16</sup>O/<sup>18</sup>O, <sup>14</sup>N/<sup>15</sup>N) in  
323 major gases compounds of Enceladus' plume, as well as <sup>12</sup>C/<sup>13</sup>C in organics contained in icy  
324 grains. Comparison of gas isotopic ratios (e.g., D/H in H<sub>2</sub>O and CH<sub>4</sub>, <sup>12</sup>C/<sup>13</sup>C in CH<sub>4</sub>, CO<sub>2</sub>,  
325 and CO; <sup>16</sup>O/<sup>18</sup>O in H<sub>2</sub>O, CO<sub>2</sub>, CO; <sup>14</sup>N/<sup>15</sup>N in NH<sub>3</sub> and N<sub>2</sub>) and with Solar System standards  
326 would provide essential constraints on the origin of volatiles and how they may have been  
327 internally reprocessed. Simultaneous precise determination of isotopic ratios in N, H, C and  
328 O- bearing species in Enceladus' plume and Titan's atmosphere would permit a better  
329 determination of the initial reference values and a quantification of the fractionation due to  
330 internal and atmospheric processes on both moons.

331 Noble gases also provide essential information on how volatiles were delivered to  
332 Enceladus and if significant exchanges between the rock phase and water-ice phase occurred  
333 during Enceladus' evolution. The E<sup>2</sup>T mission would be able to determine the abundance of  
334 <sup>40</sup>Ar, expected to be the most abundant isotope, as well as the primordial (non-radiogenic)  
335 argon isotopes, <sup>36</sup>Ar and <sup>38</sup>Ar. The detection and quantification of <sup>36</sup>Ar and <sup>38</sup>Ar would place  
336 fundamental constraints on the volatile delivery in the Saturn system. A low <sup>36</sup>Ar/N<sub>2</sub> ratio, for  
337 instance, would indicate that N<sub>2</sub> on Enceladus is not primordial, like on Titan (Niemann et al.,  
338 2010), and that the fraction of argon brought by cometary materials on Enceladus is rather  
339 low. In addition to argon, if Ne, Kr, and Xe are present in detectable amounts, E<sup>2</sup>T would be  
340 able to test whether primordial noble gases on Enceladus were primarily brought by a  
341 chondritic phase or cometary ice phase, which has implications for all the other primordial



342 volatiles. The  $^{40}\text{Ar}/^{38}\text{Ar}/^{36}\text{Ar}$  as well as  $^{20}\text{N}/^{21}\text{Ne}/^{22}\text{Ne}$  ratios would also allow for testing of  
343 how noble gases were extracted from the rocky core. Abundance ratios between Ar/Kr and  
344 Ar/Xe, if Kr and Xe are above detection limits, would offer an opportunity to test the  
345 influence of clathrate storage and decomposition in volatile exchanges through Enceladus's  
346 ice shell.

347 The origin of methane detected in Enceladus' plume is still uncertain. Methane, ubiquitous  
348 in the interstellar medium, was most likely embedded in the protosolar nebula gas. The inflow  
349 of protosolar nebular gas into the Saturn subnebula may have trapped methane in clathrates  
350 that were embedded in the planetesimals of Enceladus during their formation. Alternatively,  
351 methane may have been produced via hydrothermal reactions in Enceladus' interior; a  
352 possibility made more evident by the recent discovery of molecular hydrogen in Enceladus'  
353 plume (Waite et al., 2017). Mousis et al. (2009) suggests that if the methane of Enceladus  
354 originates from the solar nebula, then Xe/H<sub>2</sub>O and Kr/H<sub>2</sub>O ratios are predicted to be equal to  
355  $\sim 7 \times 10^{-7}$  and  $7 \times 10^{-6}$  in the satellite's interior, respectively. On the other hand, if the methane  
356 of Enceladus results from hydrothermal reactions, then Kr/H<sub>2</sub>O should not exceed  $\sim 10^{-10}$  and  
357 Xe/H<sub>2</sub>O should range between  $\sim 1 \times 10^{-7}$  and  $7 \times 10^{-7}$  in the satellite's interior. The E<sup>2</sup>T mission  
358 by performing in situ analysis with high-resolution mass spectrometry of both the vapour and  
359 solid phases would quantify the abundance ratios between the different volatile species  
360 present in the plume of Enceladus, the isotopic ratios in major species, and the noble gas  
361 abundance.

362

### 363 *3.1.2 Sources and Compositional Variability of Enceladus' Plume*

364 The detection of salty ice grains (Postberg et al., 2009, 2011), the high solid/vapour ratio  
365 (Porco et al., 2006; Ingersoll and Ewald, 2011), and the observations of large particles in the

366 lower part of the plume (Hedman et al., 2009) all indicate that the plume of Enceladus  
367 originates from a liquid source likely from the subsurface ocean rather than from active  
368 melting within the outer ice shell (Figure 3). However, the abundance of the major gas species  
369 observed by Cassini suggests some contribution from the surrounding cold icy crust should  
370 also be considered. If plume gases exclusively originate from a liquid water reservoir, low-  
371 solubility species would be more abundant than high-solubility compounds, which is not  
372 apparent in the INMS data. The saltiness of the ice grains and the recent detections of  
373 nanometer sized silica dust in E-ring particles, which are believed to come from Enceladus  
374 (Hsu et al., 2011, 2015), and molecular hydrogen in Enceladus' plume (Waite et al., 2017) all  
375 indicate their origin is a location where alkaline high temperature hydrothermal reactions and  
376 likely water-rock interactions are occurring.

### 377 FIGURE 3

378 Although the Cassini (Cosmic Dust Analyzer) CDA has constrained knowledge of plume  
379 compositional stratigraphy, measurements of the absolute abundance and composition of  
380 organics, silicates and salts are poorly constrained given the low spatial resolution (10 km),  
381 low mass resolution and limited mass range of the CDA. The E<sup>2</sup>T ENIJA is capable of  
382 providing a spatial accuracy of better than 100 m, allowing for a precise determination of  
383 compositional profiles along the spacecraft trajectory (Srama et al., 2015). The Cassini INMS  
384 provided only plume integrated spectra and is not able to separate gas species with the same  
385 nominal mass. E<sup>2</sup>T INMS' high mass resolution, which is 50 times larger than that of Cassini  
386 INMS, would allow for separation of isobaric interferences, for example separating <sup>13</sup>C and  
387 <sup>12</sup>CH and CO and N<sub>2</sub>. Determining high-resolution spatial variations in composition is crucial  
388 to establish whether the jets are fed by a common liquid reservoir or if jet sources are  
389 disconnected, and if the local liquid sources interact with a heterogeneous region in the icy  
390 crust. Variations in composition between the solid and gas phases as a function of distance

391 from jet sources can also provide information about how the less volatile species condense on  
392 the grains, thus constraining the eruption mechanisms. The E<sup>2</sup>T mission would allow for the  
393 determination of the compositional distribution between both solid and vapour phases of  
394 Enceladus' plume, thus providing crucial constraints on the nature and composition of the jet  
395 sources, and on the relative contributions of subsurface liquid reservoirs and the surrounding  
396 cold icy crust. Spatial variations in composition within the plume and possible correlations  
397 with the jet sources would permit for testing if the volatile compounds originate from a  
398 common reservoir and how the less volatile compounds are integrated in the solid particles  
399 during the eruption processes.

400

### 401 *3.1.3 Geological Constraints on Titan's Methane Cycle and Surface Evolution*

402 There is an open question whether Titan's methane-rich atmosphere is being actively  
403 replenished, or if methane is being lost and Titan's methane may eventually be depleted  
404 (Yung et al., 1984). Cryovolcanism has been suggested as a mechanism by which methane  
405 and argon can be transported from Titan's interior to its surface (e.g., Lopes et al., 2013).  
406 Cryovolcanic activity may also promote methane outgassing (Tobie et al., 2006); while  
407 methane clathrates are stable in Titan's ice shell in the absence of destabilizing thermal  
408 perturbations and/or pressure variation, variations in the thermal structure of Titan's outer ice  
409 shell during its evolution could have produced thermal destabilization of methane clathrates  
410 generating outgassing events from the interior to the atmosphere (Tobie et al., 2006; see also  
411 Davies et al., 2016). A number of candidate cryovolcanic features have been identified in  
412 Cassini observations (Lopes et al., 2013). E<sup>2</sup>T TIGER high-resolution colour images would  
413 provide the data needed to determine the genesis of these features. Stratigraphic relationships

414 and crater counting would provide a means by which the relative ages of these features may  
415 be constrained.

416 A related question to the age of Titan's atmosphere is if Titan's climate is changing. At  
417 present, most of the observed liquid methane is located in the north polar region (Aharonson  
418 et al., 2009). There have been suggestions, however, that organic seas may have existed in  
419 Titan's tropics (Moore and Howard, 2010; MacKenzie et al., 2014), and/or in broad  
420 depressions in the south (Aharonson et al., 2009; Hayes et al., 2011). Observations and  
421 models suggest Titan's methane distribution varies on seasonal timescales (e.g., Waite et al.,  
422 2007; Hayes et al., 2010; Turtle et al., 2011; Coustenis et al., 2013, 2016) or Milankovitch  
423 timescales (Aharonson et al., 2009). Alternative models suggest that methane is being  
424 depleted and Titan's atmosphere is drying out (Moore and Howard, 2010). High-resolution  
425 images of the margins and interiors of these basins would allow us to determine if they once  
426 held seas. Identification of impact features or aeolian processes within these basins would  
427 help to constrain the timing of their desiccation.

428 In addition to their inherent scientific interest, Titan's dunes serve as sensitive indicators of  
429 climatic evolution (Lorenz et al., 2006; Radebaugh et al., 2008). Larger dune forms take  
430 longer to form than smaller dune forms. In Earth's Namib desert, these differing timescales  
431 result in large, longitudinal dunes that adhere to the overall wind conditions from the  
432 Pleistocene 20,000 years ago, while smaller superposing dunes (sometimes called rake dunes,  
433 or flanking dunes) have responded to the winds during our current interglacial and orient ages  
434 accordingly (Lancaster et al., 1989). On Titan, E<sup>2</sup>T TIGER's superior spatial resolution would  
435 resolve these potential smaller dunes on top of the known longitudinal dunes, and would  
436 therefore reveal if Titan's recent climate has been stable or if it has changed over the past few  
437 Ma. The E<sup>2</sup>T mission would provide high-resolution colour imaging of Titan that can be used

438 to characterize candidate cryovolcanic features that could be replenishing Titan's atmosphere  
439 and paleo-seas, or dune patterns that evidence changes in Titan's climate.

440 Titan's geology is unique in that liquid and solid organics likely play key roles in many of  
441 the observed processes. These processes, in turn, play an important role in modifying these  
442 organics, both physically and chemically. Understanding these modification processes is  
443 crucial to investigating the complex chemistry occurring on this moon. Furthermore, study of  
444 Titan's geology allows us to investigate processes that are common on Earth, but in  
445 drastically different environmental conditions, providing a unique way to gain insight into the  
446 processes that shaped the Earth and pre-Noachian Mars.

447 Observations of Titan suggest the landscape is significantly modified by liquid organics  
448 (e.g., Tomasko et al., 2005; Soderblom et al., 2007; Burr et al., 2013). Fluvial erosion is  
449 observed at all latitudes, with a variety of morphologies suggesting a range of controls and  
450 fluvial processes (Burr et al., 2013). High-resolution color imaging would provide insight into  
451 the nature of this erosion: whether it is predominantly pluvial or sapping in nature and  
452 whether it is dominated by mechanical erosion or dissolution. Dissolution processes are also  
453 suspected to control the landscape of Titan's labyrinth terrains (Cornet et al., 2015) and may  
454 be responsible for the formation of the polar sharp edged depressions (Hayes et al., 2008):  
455 E<sup>2</sup>T imaging would allow direct testing of these hypotheses.

456 Both fluvial and aeolian processes likely produce and transport sediments on Titan. Dunes  
457 are observed across Titan's equator (e.g., Radebaugh et al., 2008; Malaska et al., 2016) while  
458 a variety of fluvial sediment deposits have been identified across Titan (e.g., Burr et al., 2013;  
459 Birch et al., 2016). Detailed images of the margins of the dune fields would allow us to  
460 determine the source and fate of sands on Titan. E<sup>2</sup>T images would also help determine  
461 whether the observed fluvial features are river valleys or channels (cf. Burr et al., 2013)

462 providing key information in obtaining accurate discharge estimates needed to model  
463 sediment transport (Burr et al., 2006). E<sup>2</sup>T observation would provide insight into the primary  
464 erosion processes acting on crater rims, which likely comprise a mixture of organics and  
465 water ice (cf. Neish et al., 2015, 2016). Finally, E<sup>2</sup>T images may provide insight into the  
466 nature of erosion that exists in Titan's mid-latitudes, a region that shows little variability in  
467 Cassini observations.

468 Of great interest in understanding the evolution of Titan's surface is determining the nature  
469 of the observed geologic units, including their mechanical and chemical properties. Fluvial  
470 processes, the degree to which mechanical versus dissolution dominates and the existence of  
471 sapping, reflect the material properties of the surface and therefore can be used as a powerful  
472 tool to investigate the properties of the surface. E<sup>2</sup>T imaging would also allow us to  
473 investigate the strength of the surface materials by constraining the maximum slopes  
474 supported by different geologic units. Detailed color and stereo imaging of the boundaries of  
475 units would also allow investigation of the morphology, topography, and spectral relationship  
476 across unit boundaries. E<sup>2</sup>T would take high-resolution color images of Titan that would  
477 elucidate the nature of the geological evolution of Titan's organic-rich surface.

478

## 479 **3.2 Habitability and Potential for Life in Ocean Worlds, Enceladus and Titan**

### 480 **3.2.1 Evidence for Prebiotic and Biotic Chemical Processes on Titan and Enceladus**

481 Unlike the other ocean worlds in the Solar System, Titan has a substantial atmosphere,  
482 consisting of approximately 95% nitrogen and 5% methane with trace quantities of  
483 hydrocarbons such as ethane, acetylene, and diacetylene, and nitriles, including hydrogen  
484 cyanide (HCN) and cyanogen (C<sub>2</sub>N<sub>2</sub>). Somewhat more complex molecules such as  
485 cyanoacetylene, vinyl and ethylcyanide follow from these simpler units. In Titan's upper

486 atmosphere, Cassini has detected large organic molecules with high molecular masses over  
487 100 u. In-situ measurements by the Cassini Plasma Spectrometer (CAPS) detected heavy  
488 positive ions (cations) up to 400 u (Crary et al., 2009) and heavy negative ions (anions) with  
489 masses up to 10,000 u (Coates et al., 2007) in Titan's ionosphere. Whereas Cassini INMS  
490 only had the ability to detect cations, E<sup>2</sup>T INMS can detect both cations and anions and can  
491 do so with much better mass resolution than Cassini-INMS (and a fortiori than Cassini-  
492 CAPS). It is thought that these heavy negative ions, along with other heavy molecules found  
493 in the upper atmosphere, are likely the precursors of aerosols that make up Titan's signature  
494 orange haze, possibly even precipitating to the surface. While the compositions of these  
495 molecules are still unknown, their presence suggest a complex atmosphere that could hold the  
496 precursors for biological molecules such as those found on Earth. The ability to detect  
497 prebiotic molecules in Titan's atmosphere is currently limited by the mass range of the  
498 Cassini INMS to the two smallest biological amino acids, glycine (75 u) and alanine (89 u),  
499 and the limited mass resolution precludes any firm identification. While Cassini INMS has  
500 not detected 75 or 89 u molecules, it has detected positive ions at masses of 76 u and 90 u,  
501 which are consistent with protonated glycine and alanine, respectively (Vuitton et al., 2007;  
502 Hörst et al., 2012). Experimental results from a Titan atmosphere simulation experiment  
503 found 18 molecules that could correspond to amino acids and nucleotide bases (Hörst et al.,  
504 2012). The E<sup>2</sup>T mission would use high-resolution mass spectrometry to measure heavy  
505 neutral and ionic constituents up to 1000 u, and the elemental chemistry of low-mass organic  
506 macromolecules and aerosols in Titan's upper atmosphere, and would monitor neutral-ionic  
507 chemical coupling processes.

508 The plume emanating from Enceladus' south pole probably contains the most accessible  
509 samples from an extra-terrestrial liquid water environment in the Solar System. The plume is  
510 mainly composed of water vapour and trace amounts of other gases (Waite et al., 2017). In

511 addition, higher molecular weight compounds with masses exceeding 100 u, were detected in  
512 the plume emissions (Waite et al., 2009; Postberg et al., 2015). The presence of CO<sub>2</sub>, CH<sub>4</sub> and  
513 H<sub>2</sub> can constrain the oxidation state of Enceladus' hydrothermal system during its evolution.  
514 The minor gas constituents in the plume are indicative of high-temperature oxidation-  
515 reduction (redox) reactions in Enceladus' interior possibly a result of decay of short-lived  
516 radionuclides (Schubert et al., 2007). In addition, H<sub>2</sub> production and escape may be a result  
517 of redox reactions indicative of possible methanogenesis similar to the process occurring in  
518 terrestrial submarine hydrothermal vents (McKay et al., 2008; Waite et al., 2017). Further, the  
519 high temperatures and H<sub>2</sub> escape may have led to the oxidation of NH<sub>3</sub> to N<sub>2</sub> (Glein et al.,  
520 2008). Detection and inventory of reduced and oxidized species in the plume material (e.g.,  
521 NH<sub>3</sub>/N<sub>2</sub> ratio, H<sub>2</sub> abundance, reduced versus oxidized organic species) can constrain the redox  
522 state and evolution of Enceladus' hydrothermal system.

523 Cassini CDA measurements identified three types of grains in the plume and Saturn's E-ring.  
524 Type I and Type II grains are both salt-poor (Figure 4). Type I ice grains are nearly pure-  
525 water ice while Type II grains also possess silicates and organic compounds and Type III  
526 grains are salt-rich (0.5–2.0% by mass) (Postberg et al., 2009, 2011). The salinity of these  
527 particles, the high solid/vapor ratio (Porco et al., 2006, Ingersoll and Ewald, 2011) of the  
528 plume and observations of large particles in the lower part of the plume (Hedman et al., 2009)  
529 indicate that the plume originates from a subsurface liquid source. The Cassini CDA later  
530 detected nanometer sized silica dust particles in E-ring stream particles (Hsu et al., 2011,  
531 2015) which indicate that water-rock interactions are likely taking place within this liquid  
532 reservoir. Gravity and libration data demonstrated that this liquid reservoir was a subsurface  
533 global ocean (Iess et al., 2014; Thomas et al., 2015)

534 **FIGURE 4**



535 Hsu et al. (2015) suggest that the ocean should be convective in order to have silica  
536 nanoparticles transported from hydrothermal sites at the rocky core up to the surface of the  
537 ocean where they can be incorporated into icy plume grains (Hsu et al., 2015). To confirm  
538 this hypothesis of current hydrothermal activity on Enceladus, a direct detection of silica and  
539 other minerals within ejected ice grains is required. SiO<sub>2</sub> nano-particles detected in Saturn's  
540 E-ring could be much better investigated and quantified by E<sup>2</sup>T ENIJA given its high dynamic  
541 range (10<sup>6</sup>–10<sup>8</sup>). By performing high-resolution mass spectrometry of ice grains in Enceladus'  
542 plume, the E<sup>2</sup>T mission would characterize the composition and abundance of organics, salts  
543 and other minerals embedded in ice grains, as messengers of rock/water interactions. It would  
544 also search for signatures of on-going hydrothermal activities from possible detection of  
545 native He and further constrain recent measurements of native H<sub>2</sub> found in Enceladus' plume  
546 (Waite et al., 2017).

547

### 548 **3.2.2 Physical Dynamics in Enceladus' Plume and Links to Subsurface Reservoirs**

549 The total heat emission at Enceladus' tiger stripes is at least 5 GW - possibly up to 15 GW,  
550 (Howett et al., 2011), and in some of the hot spots where jets emanate, the surface  
551 temperatures are as high as 200 K (Goguen et al., 2013). Cassini observations show that the  
552 plume is made up of approximately 100 discrete collimated jets as well as a diffuse  
553 distributed component (Hansen et al., 2008, 2011; Postberg et al., 2011; Porco et al., 2014).  
554 The majority of plume material can be found in the distributed diffuse portion of the plume,  
555 which likely originates from elongated fissures along Enceladus' tiger stripes while only a  
556 small portion of gas and grains are emitted from the jets (Hansen et al., 2011; Postberg et al.,  
557 2011). CDA measurements demonstrate that the majority of salt-poor grains tend to be ejected  
558 through the jets and at faster speeds while larger salt-rich grains tend to be ejected more

559 slowly through the distributed portion of the plume (Postberg et al., 2011). The ice to vapour  
560 ratio can constrain how Enceladus' plume material is formed and transported to the surface.  
561 For example, ice/vapour ratios  $> 0.1$ – $0.2$  would exclude plume generation mechanisms that  
562 require a large amount of ice grains to be condensed from vapour (Porco et al., 2006;  
563 Ingersoll and Pankine, 2011). However, this ratio is poorly constrained with estimates ranging  
564 from 0.05 (Schmidt et al., 2008) to 0.4 (Porco et al., 2006) to 0.35–0.7 (Ingersoll and Ewald,  
565 2011). E<sup>2</sup>T high-resolution IR images and ENIJA can help constrain this important ratio.  
566 Cassini ISS images used to track plume brightness variation, which is proportional to the  
567 amount of grains in the plume, with the orbital position of Enceladus found more ice grains  
568 are emitted when Enceladus is near its farthest point from Saturn (apocenter). It is not  
569 understood if the plume vapour has such a variation. This temporal variation of the plume  
570 indicates that it is tidally driven but could also be due to possible physical libration (Hurford  
571 et al., 2009; Kite et al., 2016). Most recently, Kite et al. (2016) has suggested that the tiger  
572 stripe fissures are interspersed with vertical pipe-like tubes with wide spacing that extend  
573 from the surface to the subsurface water. This mechanism allows tidal forces to turn water  
574 motion into heat, generating enough power to produce eruptions in a sustained manner.  
575 TIGER can provide high spatial resolution thermal emissions maps to constrain the amount of  
576 energy dissipated between the tiger stripes. The E<sup>2</sup>T mission would use high resolution IR  
577 imaging of the south polar terrain and mass spectra of the grains to provide new details of its  
578 surface and constrain the links between plume activity, subsurface reservoirs and deep  
579 hydrothermal processes.

580

581

582

### 583 3.2.3 Geological Evidence for Interior-Surface Communication on Titan

584 Geological processes such as tectonism and cryovolcanism indicate communication between  
585 the surface and subsurface. While Titan's surface offers a wealth of geological processes, the  
586 Cassini data lack the resolution needed in which to constrain the detailed nature of these  
587 processes, and thus to understand the extent that Titan's surface may be chemically  
588 interacting with its water-rich interior. Also of great importance to habitability are the  
589 transient H<sub>2</sub>O melt sheets and flows (e.g., Soderblom et al., 2010) associated with impacts. On  
590 Titan, several features with volcanic landforms, lengthy flows, tall mountains, large caldera-  
591 like depressions, have been identified as possible cryovolcanic sites but could also possibly be  
592 due to other endogenic processes (Lopes et al., 2016; Solomonidou et al., 2016). At present,  
593 the Hotei Regio flows and the Sotra Patera region, which includes Sotra Patera, an elliptical  
594 deep depression on Titan, Mohini Fluctus, a lengthy flow feature, and Doom and Erebor  
595 Montes, two volcanic edifices, are considered to host the strongest candidates for  
596 cryovolcanism on Titan (Lopes et al., 2013; Solomonidou et al., 2014, 2016).

597 A variety of mountainous topography has been observed on Titan (Radebaugh et al., 2007;  
598 Cook-Hallett et al., 2015). The observed morphologies of many of Titan's mountains suggest  
599 contractional tectonism (Mitri et al., 2010; Liu et al., 2016). This is somewhat surprising,  
600 however, since tectonic landforms observed on other ocean worlds and icy satellites in the  
601 outer solar system appear to be extensional in nature. Understanding Titan's tectonic regime  
602 would, thus not only provide insight into the transport of material between surface and the  
603 interior, but also into the evolution of the other ocean worlds. We would test the hypothesis  
604 that Titan's mountains are formed by contraction by mapping the faults driving mountain  
605 formation in topographic context. The shape of the fault outcrop draped against topography  
606 would allow us to measure the dips of faults, which would be ~30 degrees to the horizontal  
607 for compressive mountains and ~60 degrees for extensional mountains.

608 In addition to cryovolcanism and tectonism, which may transport water to Titan's surface,  
609 impact craters likely have created transient liquid-water environments on Titan's surface.  
610 Because of Titan's dense atmosphere, models suggest that melt sheets and flows associated  
611 with impact craters may remain liquid for  $10^4$ – $10^6$  years (Thompson and Sagan, 1992;  
612 Artemieva and Lunine, 2005), though the stability of such melts is questioned (Senft and  
613 Stewart, 2011; Zahnle et al., 2014) and detailed imaging of the floors of young craters is  
614 needed to constrain these models. Titan offers numerous pathways for interaction between its  
615 organic-rich surface and liquid water. E<sup>2</sup>T would provide high-resolution mapping (30  
616 m/pixel with DTM vertical resolution of 10 m) that would offer the ability to distinguish  
617 cryovolcanic features and to investigate the morphology of Titan's mountains and impact  
618 craters.

619

#### 620 **4. Scientific Payload**

621 The Explorer of Enceladus and Titan (E<sup>2</sup>T) has a focused payload that would provide in-situ  
622 mass spectrometry and high-resolution imaging of Enceladus' south polar terrain and plume,  
623 and Titan's upper atmosphere and surface, from a solar-electric powered spacecraft in orbit  
624 around Saturn. The in-situ measurements of Titan's upper atmosphere would be acquired  
625 during 17 flybys with an altitude as low as 900 km. At Enceladus, in-situ measurements  
626 would be conducted during 6 flythroughs of the plume and flybys of the south polar terrain at  
627 altitudes between 50 and 150 km. At the closest approach the velocity of the S/C with respect  
628 to Enceladus surface is ~5 km/s and with respect to Titan surface is ~7 km/s. Imaging data  
629 will be collected during inbound and outbound segments of each flyby.

630 The E<sup>2</sup>T mission model payload consists of three science instruments: two time-of-flight  
631 mass spectrometers, the Ion and Neutral gas Mass Spectrometer (INMS) and the Enceladus

632 Icy Jet Analyzer (ENIJA); and a high-resolution infrared camera, Titan Imaging and Geology,  
633 Enceladus Reconnaissance (TIGER). Two instruments in the E<sup>2</sup>T payload were proposed to  
634 be provided by ESA member states. INMS would be provided by the Swiss Space Office  
635 (SSO) and ENIJA would be provided by the German Aerospace Center (DLR). NASA  
636 proposed to provide the third instrument, TIGER. The characteristics of the science payload  
637 are shown in Table 2. In addition, a Radio Science Experiment (RSE), not necessarily  
638 requiring specific hardware on-board the spacecraft – thus regarded as an “experiment of  
639 opportunity”, was considered for further study. The RSE would improve the current  
640 determination of the gravity fields of Enceladus and Titan, by using the radio links between  
641 the E<sup>2</sup>T spacecraft and Earth to better constrain their internal structure. The proposed main  
642 funding agency of the RSE is the Italian Space Agency (ASI).

TABLE 2

#### 645 **4.1 Ion and Neutral Mass Spectrometer (INMS)**

646 The Ion and Neutral Mass Spectrometer (INMS) is a reflectron time-of-flight mass  
647 spectrometer that would record mass spectra of neutral and ionised gases during flybys and  
648 fly-throughs of Enceladus’ plume and Titan’s upper atmosphere. During flybys and  
649 flythroughs of Saturn’s E-ring, Enceladus’ plume and of Titan’s upper atmosphere, INMS  
650 would record mass spectra of neutral, positive and negative ionized gases within the mass  
651 range 1 – 1000 u/e with a mass resolution at 5000 m/ $\Delta$ m (50%) and a sensitivity (detection  
652 threshold) of 1 cm<sup>-3</sup> ( $\sim 10^{-16}$  mbar) in a 5 s measurement cadence (Abplanalp et al., 2010;  
653 Wurz et al., 2012). The Cassini INMS (Ion and Neutral Mass Spectrometer) is limited to the  
654 detection of low mass species of 1–99 u and is therefore not able to measure the high-mass  
655 molecular species abundant in Enceladus’ plume and in Titan’s upper atmosphere. Further,

656 E<sup>2</sup>T INMS' high mass resolution ( $m/\Delta m = 5000$ ), 50 times larger than Cassini INMS, allows  
657 for the separation of isobaric interference such as occur at masses 16, 20, 28, and 40 u/e  
658 which is possible based on heritage of RTOF/ROSINA from the Rosetta mission (Scherer et  
659 al., 2006; Wurz et al., 2015) as shown in Figure 5.

## FIGURE 5

661 Cassini INMS only had the ability to measure positively charged ions. In-situ  
662 measurements by the Cassini Plasma Spectrometer (CAPS) detected heavy negative ions in  
663 Titan's ionosphere and negative water group ions in Enceladus' plume (Coates et al., 2010).  
664 E<sup>2</sup>T INMS would record 10,000 mass spectra per second and accumulate these for a pre-set  
665 period, allowing for a time resolution of measurements in the range from 0.1 to 300 s. The  
666 maximum INMS time resolution at Enceladus is 0.1 s for recording a mass spectrum  
667 (corresponding to a spatial resolution of  $\sim 0.5$  km for a S/C velocity of 5 km/s) to resolve  
668 small-scale structure in the plume; the maximum used INMS resolution at Titan is 5 s  
669 (corresponding to a spatial resolution of  $\sim 35$  km for a S/C velocity of 7 km/s).

670 The E<sup>2</sup>T INMS has heritage based on P-BACE instrument (Abplanalp et al., 2009.), RTOF  
671 instrument of ROSINA (Scherer et al., 2006) on Rosetta and on the gas-chromatograph-  
672 neutral gas mass spectrometer prototype which will be used in upcoming lunar exploration  
673 conducted by the Russian Space Agency in 2019 (Hofer et al., 2015; Wurz et al., 2015). Most  
674 recently, a similar instrument, the Neutral gas and Ion Mass spectrometer (NIM) instrument  
675 of the Particle Environment Package (PEP) consortium, is developed for the JUICE mission  
676 of ESA.

677

678

## 679 **4.2 Enceladus Icy Jet Analyzer (ENIJA)**

680 Enceladus Icy Jet Analyzer (ENIJA) is optimized to search for prebiotic molecules and  
681 biogenic compounds in objects with high dust fluxes and number densities such as occur in  
682 Enceladus' plume or cometary comae. ENIJA consists of two time-of-flight mass  
683 spectrometer subsystems and a software-enabled high flux detector (HFD) that runs in parallel  
684 to the spectrometers. The high flux detector measurement mode will map the dynamical  
685 profile (number density and size distribution) of Enceladus' ice jets. Compared to the Cassini  
686 CDA (Cosmic Dust Analyzer), ENIJA has a 40 times better mass resolution, a 100 times  
687 better maximum flux and sensitivity, and a spatial resolution that is 50 times better (Srama et  
688 al., 2004, 2015; Postberg et al., 2009). Moreover, the twin-detector instrument will acquire  
689 mass spectra of both cations and anions created upon ice particle impact, simultaneously,  
690 whereas CDA only measured cations. During flythroughs of Enceladus plume and in the E  
691 ring, ENIJA provides time-of-flight mass spectra for ice particles with a mass range of 1–  
692 2000 u with a mass resolution ( $m/\Delta m$ ) of 970 between 23-2000 u. ENIJA acquires time-of-  
693 flight mass spectra of individual ice grains by impact ionization and analyses the generated  
694 anions and cations with two separate time of flight spectrometer sub-units. In this way ENIJA  
695 is able to quantify organic compounds at <10 ppm; additionally some polar organic species,  
696 such as most amino acids, can be quantified well below 1 ppm (Figure 6). With a dynamic  
697 range up to  $10^8$ , inorganic trace components with sub-ppm concentrations from Enceladus'  
698 ocean, can now be investigated simultaneously with the more abundant mineral species.  
699 ENIJA is not a newly developed instrument; rather it is an optimization and miniaturization of  
700 flight-proven hardware. ENIJA has heritage based on Giotto-Particle Impact Analyzer (PIA),  
701 Stardust Cometary Interstellar Dust Analyzer (CIDA), Cassini's' Cosmic Dust Analyzer  
702 (CDA), Rosetta COmetary Secondary Ion Mass Analyzer (COSIMA) and Europa-SURface  
703 Dust mass Analyzer (SUDA).

704

FIGURE 6

705

**706 4.3 Titan Imaging and Geology, Enceladus Reconnaissance (TIGER)**

707 Titan Imaging and Geology, Enceladus Reconnaissance (TIGER) is a near infrared (NIR)  
708 camera designed to acquire high resolution images of Titan and Enceladus. TIGER would  
709 observe Titan at 30–100 m/pixel in three wavelengths, 1.3, 2, and 5  $\mu\text{m}$  and Enceladus  
710 emissions at 1 m/pixel at two wavelengths, 5 and 5.3  $\mu\text{m}$ . Images acquired by TIGER would  
711 enable investigation of Titan's geology, hydrology, and compositional variability and study of  
712 the composition and kinematics of Enceladus' jets and plumes. The TIGER band passes are  
713 selected to match with Titan's atmospheric transmission windows (Lemmon et al., 1993;  
714 Sotin et al., 2005) to enable direct ground observations using reflected sunlight and to  
715 measure thermal emission from Enceladus. The 5  $\mu\text{m}$  images are subject to virtually no  
716 scattering from Titan's atmospheric aerosols, allowing diffraction limited images achieving  
717 spatial resolutions an order of magnitude better than Cassini observations (Clark et al., 2010;  
718 Soderblom et al., 2012; Barnes et al., 2014) and would be highly sensitive to organic  
719 composition (Clark et al., 2010; Barnes et al., 2014). TIGER has the capability to image Titan  
720 at Huygens DISR resolution (Figure 7). At Enceladus, the 5 and 5.3  $\mu\text{m}$  observations would  
721 measure thermal emission of surfaces as cold as 130 K and would provide temperature maps  
722 of the surface at Cassini-ISS image scales. A fine steering mirror (FSM) would be employed  
723 to select and track regions of interest during the flyby and compensate for spacecraft jitter  
724 allowing for longer exposures and better signal-to-noise ratio (SNR). Digital time-delay  
725 integration (TDI) would also be employed, as needed, during closest approach when the  
726 ground speed is highest.

727

FIGURE 7



728 While the TIGER instrument is a new design, it utilizes high-heritage subsystems with a  
729 Technology Readiness Level (TRL) larger of 6. The TIGER Focal Plane Array (FPA) is from  
730 Teledyne Imaging Sensors and utilizes the same HgCdTe detector and H2RG qualified for  
731 James Webb Space Telescope (JWST) Near Infrared Camera (NIRCam) (Rieke et al., 2005),  
732 Near Infrared Spectrometer (NIRSpec) (Rauscher et al., 2004), and Fine Guidance Sensor  
733 (FGS) (Doyon et al., 2012) instruments. TIGER also implements FPA readout electronics that  
734 have been qualified extensively for the JWST instruments (Loose et al., 2006) and are used by  
735 the Euclid Near Infrared Spectrometer and Photometer (NISF) (Maciaszek et al., 2014).

736

#### 737 **4.4 Radio Science Experiment**

738 Gravity field measurements are powerful tools to constrain the interior structure of the planets  
739 and satellites and to assess mass anomalies, providing information on the internal dynamics  
740 and evolution. The observable quantities used by gravity science experiments are obtained by  
741 means of spacecraft tracking at microwave frequencies from a terrestrial ground antenna. The  
742 eight gravity flybys of Titan conducted by the Cassini mission (not including the T122 flyby,  
743 recently completed in August 2016) yielded sufficient information to obtain a robust  
744 estimation of the degree-3 static gravity field, plus the fluid Love number  $k_2$  (Iess et al., 2010,  
745 2012); however, this was not the case for Enceladus (Rappaport et al., 2008; Iess et al., 2014),  
746 where only the degree-2 static gravity field and  $J_3$  were observed, and the tidal response to  
747 Saturn's gravity was not detected.

748 In Enceladus' south polar terrain a larger time-variation of the gravity field with respect to  
749 the global solution of the time variation of the gravity field is expected because the ice shell  
750 thickness is anticipated to be locally thin in that area. A gravity science experiment, based on  
751 radio tracking and precise spacecraft multiarc orbit determination (see e.g. Tortora et al.,

2016), would determine the local solution of the gravity field of Enceladus at the south polar terrain thus allowing the determination of the thickness variation at the south polar regions and constraining the mechanical properties (viscosity) of the ice overlying the outer ice shell. The expected tidal deformation is characterized by a pattern more complex than the standard degree-two pattern, with a strong amplification of the tidal fluctuation in the south polar terrain (Behoukova et al., 2017).

For Titan gravity science, a desirable objective would be the improve of Cassini's results in terms of reduction of the uncertainty in the fluid Love number  $k_2$ . In particular, the geophysics objectives relative to the subsurface liquid ocean extent, shell thickness and shell viscosity would be improved if the formal uncertainty of  $k_2$  could be reduced down to values in the range 0.05-0.01. The feasibility of such result strongly depends on the actual geometry of Titan's flyby (in particular: altitude at pericenter and mean anomaly of Titan around Saturn at the time of closest approach with the E<sup>2</sup>T spacecraft), in addition to the stability of the radio link (preferably at Ka-band, to reduce the detrimental effect of dispersive media).

The availability of a two-way (uplink and downlink) radio system would also allow expanding the long series of Titan's occultations carried out by Cassini's radio science subsystem to probe Titan's neutral and ionized atmosphere (Coustenis et al., 2016; Kliore et al., 2008, 2011; Schinder et al., 2012, 2015). The main objective would be the characterization of Titan's atmospheric structure (pressure, density, and total electron content profiles, versus altitude) at different latitude/longitudes.

772

## 773 **5. Proposed Mission and Spacecraft Configuration**

774 The baseline scenario for the E<sup>2</sup>T mission is a solar electric powered spacecraft (S/C), in orbit  
775 around Saturn, performing multiple flybys of Titan and Enceladus. The baseline includes a

776 shared launch on the Ariane 6.4 with a co-manifest of estimated launch mass of ~2636 kg to  
777 geosynchronous transfer orbit (GTO), with a forecasted shared launch opportunity in 2030.  
778 The Ariane 6.4 with four solid rocket boosters is scheduled to debut in 2020–2021. The upper  
779 stage reignition capability of the Ariane 6.4 will enable a GTO/escape dual launch. The mass  
780 estimate for the co-manifest places it in the lower end of the Intermediate Class (2,500-4,200  
781 kg) of commercial satellites (FAA, 2015). After a transfer from GTO to a hyperbolic escape  
782 trajectory, E<sup>2</sup>T S/C would pursue a gravity assist flyby of the Earth to help propel itself to the  
783 Saturn system. The cruise phase from Earth to Saturn would be 6 years long. The E<sup>2</sup>T tour in  
784 the Saturn system would be 3.5 years long. The E<sup>2</sup>T tour consists of 6 flybys of Enceladus  
785 above the south polar terrain with a flight altitude range between 50 to 150 km, and 17 flybys  
786 of Titan at a reference flight altitude ranging from 1500 down to 900 km.

787

## 788 **5.1 Transfer Orbit to Saturn**

789 The nominal transfer to Saturn uses a 1:1<sup>+</sup> resonant Earth flyby trajectory, as shown in Table  
790 3 and Figure 8. Electric propulsion is used to strongly increase the hyperbolic flyby speed at  
791 the Earth, and to provide a subsequent energy boost to reduce the total flight time to 6 years to  
792 Saturn orbit insertion (SOI). After separation from the co-manifested satellite and the  
793 SYstème de Lancement Double Ariane (SYLDA) carrier, the upper stage will be re-ignited  
794 near perigee to impart approximately 1.2 km/s  $\Delta V$  to the E<sup>2</sup>T S/C, putting it on a hyperbolic  
795 escape trajectory with a characteristic energy ( $C_3$ ) of 9.6 km<sup>2</sup>/s<sup>2</sup>. Thanks to the use of electric  
796 propulsion and an Earth gravity assist, the declination of the asymptote can vary between  $\pm 5$   
797 degrees without significant propellant mass penalty. Similarly, as shown in Table 4, there is  
798 negligible performance variation over a 21-day launch period. The data in Table 3 is based on  
799 a proposed launch from January-May 2030 during which there is little variation in flight time  
800 or required propellant mass. Lunar flybys on the escape trajectory were not considered, but

801 could be used to effectively lower the required escape  $\Delta V$ , which in turn would allow for a  
802 heavier co-manifested satellite.

803 FIGURE 8

804 TABLE 3

805 TABLE 4

806

## 807 **5.2 Saturn Tour**

808 The duration of the tour from SOI through to the end of the 17-flyby Titan phase is about 3.5  
809 years. A sample tour is shown in Figure 9. Like Cassini, end-of-mission spacecraft disposal is  
810 Saturn impact, by means of three to four additional Titan flybys.

811 The tour is divided in a first Enceladus science phase and in a second Titan science phase.  
812 The S/C should perform at least 6 flybys of Enceladus above the south polar terrain and at  
813 least 17 flybys of Titan. To prevent contamination from Titan's organics for Enceladus  
814 science, E<sup>2</sup>T S/C will perform close flybys of Enceladus at the beginning of the tour  
815 (Enceladus science phase); distant flybys of Titan would be performed during the initial tour  
816 phase. After the main Enceladus phase, close flybys of Titan with atmospheric sampling  
817 would be performed (Titan science phase).

818 FIGURE 9

819 During Enceladus science phase, E<sup>2</sup>T would provide in-situ sampling of the plume at a  
820 minimum altitude from Enceladus' surface ranging between 50 and 150 km using INMS and  
821 ENIJA. At the closest approach, the velocity of the S/C with respect to Enceladus' surface  
822 will be approximately 5 km/s. E<sup>2</sup>T would provide high-resolution imaging of Enceladus

823 surface with the TIGER camera. During Enceladus flybys the observations of INMS, ENIJA  
824 and TIGER would be performed simultaneously. During this phase observations of Titan's  
825 surface using TIGER are scheduled during distant flybys.

826 During the Titan science phase, E<sup>2</sup>T would provide in-situ sampling of the upper  
827 atmosphere at a minimum altitude from Titan surface as low as 900 km using INMS. At the  
828 closest approach the velocity of the S/C with respect to Titan's surface will be approximately  
829 7 km/s. E<sup>2</sup>T will provide high-resolution imaging of Titan's surface with TIGER camera.  
830 During Titan flybys the observations of INMS and TIGER can be performed simultaneously.

831

### 832 **5.3 Spacecraft Design and Structure**

833 The proposed E<sup>2</sup>T spacecraft (S/C) design is the result of the harmonisation of several high-  
834 TRL key space technologies already developed on behalf of several ESA space exploration  
835 missions, such as: ExoMars 2016, JUICE, BepiColombo and Rosetta. The proposed E<sup>2</sup>T  
836 spacecraft architecture would be derived from the ESA ExoMars Trace Gas Orbiter (TGO)  
837 developed for the 2016 mission. The proposed E<sup>2</sup>T architecture is in compliance with the  
838 Ariane 6.4 launcher size constraints. Table 5 summarizes its main technical characteristics.  
839 The E<sup>2</sup>T spacecraft baseline configuration is depicted in Figure 10.

840

TABLE 5

841

FIGURE 10

842 The Solar Arrays (SA) are the main S/C electrical power source, whereas the S/C main  
843 battery provides the emergency backup one. The E<sup>2</sup>T four panel solar arrays are based on  
844 space-qualified Thales Alenia Space SolarBus W51 technologies and GaAs/Ge Low Intensity  
845 Low Temperature (LILT) solar cells technology used in the ESA JUICE mission. The Solar

846 Electric Propulsion System (SEPS) is based on four (3+1 for redundancy) QinetiQ's T6  
847 gridded ion thruster engines, whereas two chemical propulsion systems have been also  
848 implemented for S/C manoeuvres and Attitude and Orbital Control System (AOCS) purposes.  
849 The propulsion systems' designs have been directly derived from different mission heritages,  
850 such as the two ESA missions GOCE and BepiColombo, and the NASA/ESA/ASI Cassini  
851 mission. The heritage of systems and subsystems from previous ESA missions requiring  
852 limited technological development enables a relatively low cost for the industrial  
853 development. The E<sup>2</sup>T S/C design was performed by Thales Alenia Space (TAS-I, Torino,  
854 Italy)

855

## 856 **6. Summary**

857 The previous decades have seen a revolution in our understanding of ocean worlds thanks in  
858 part to the Cassini-Huygens mission. Recent space missions to the outer Solar System have  
859 shown that liquid water once thought to be confined to Earth is quite common in the Solar  
860 System. The finding of subsurface oceans on Titan and Enceladus increases the possibility of  
861 extra-terrestrial habitability since life as we know it requires water, energy and nutrients  
862 (McKay et al., 2008, 2016). The geological activity represented by the eruptions forming  
863 Enceladus' plume at its south polar terrain and the organic-rich atmosphere and geological  
864 landscape, including lakes and seas, on Titan provide an ideal laboratory to investigate  
865 processes that may have been operational in Earth's early history.

866 Scientific investigations at both Titan and Enceladus as well as terrestrial experiments  
867 replicating conditions found on the icy moons have hinted at the real possibility of prebiotic  
868 activity on these icy ocean worlds. The ability to detect prebiotic molecules in Titan's  
869 atmosphere is currently limited by the mass range of the Cassini INMS to the two smallest

870 biological amino acids, glycine (75 u) and alanine (89 u), and the limited mass resolution  
871 precludes any firm identification. However, the recent detection of prebiotic chemicals  
872 (glycine and phosphorus) in comet Churyumov/Gerasimenko (Altwegg et al., 2016) makes it  
873 likely that prebiotic molecules could be also present in Enceladus' plumes. Experimental  
874 results from a Titan atmosphere simulation experiment found 18 molecules that could  
875 correspond to amino acids and nucleotide bases (Hörst et al., 2012). The E<sup>2</sup>T mission would  
876 use high-resolution mass spectrometry to measure heavy neutral and ionic constituents up to  
877 1000 u, and the basic chemistry of low-mass organic macromolecules and aerosols in Titan's  
878 upper atmosphere, and would monitor neutral-ionic chemical coupling processes.

879 Investigations of Enceladus' plume emissions has yielded tantalizing information which  
880 are suggestive of prebiotic/biotic activity, including the detection of higher molecular weight  
881 compounds with masses exceeding 100 u, (Waite et al., 2009; Postberg et al., 2015) and  
882 minor gas constituents in the plume that are indicative of high-temperature oxidation-  
883 reduction (redox) reactions in Enceladus' interior. Recent detection of molecular hydrogen in  
884 Enceladus' plume by Cassini could indicate processes that are similar in nature to processes  
885 that occur in terrestrial submarine hydrothermal vents which emit large quantities of  
886 molecular hydrogen due to water-rock interactions. In these hydrothermal vents, molecular  
887 hydrogen serves as a fuel that supports both abiotic and biotic production of organic  
888 molecules that have been detected in Enceladus' plume (Waite et al., 2015, 2017). Detection  
889 and inventory of reduced and oxidized species in the plume material (e.g., NH<sub>3</sub>/N<sub>2</sub> ratio, H<sub>2</sub>  
890 abundance, reduced versus oxidized organic species) such as proposed by the E<sup>2</sup>T mission  
891 could constrain the redox state and evolution of Enceladus' hydrothermal system.

892 Another key question still to be resolved is to understand how the plume is generated.  
893 E<sup>2</sup>T's imaging system could provide high spatial resolution thermal emissions maps to  
894 constrain the amount of energy dissipated between the tiger stripes. The E<sup>2</sup>T mission would

895 use high resolution infrared imaging of the south polar terrain and mass spectra of the grains  
896 to provide new data of its surface to constrain the links between plume activity, subsurface  
897 reservoirs and deep hydrothermal processes.

898 While Titan's surface offers a wealth of geological processes, the Cassini data lack the  
899 resolution necessary to constrain the detailed nature of these processes. E<sup>2</sup>T would provide  
900 high-resolution mapping (30 m/pixel with DTM vertical resolution of 10 m) that would offer  
901 the ability to distinguish geological features and morphology. Further, the high-resolution  
902 imaging of Titan's surface could improve understanding of the extent that Titan's organic-rich  
903 surface may be chemically interacting with its water-rich interior. By combining in-situ  
904 chemical analysis of Titan's atmosphere and Enceladus' plume with observations of  
905 Enceladus' plume dynamics and Titan's surface geology, E<sup>2</sup>T will be able to address  
906 fundamental science questions that would relate to content, origin and evolution of ocean  
907 worlds. The science that a mission such as E<sup>2</sup>T can provide can also answer questions about  
908 Earth's early history as well as help to predict the physical and chemical properties of  
909 exoplanets beyond the Solar System.

910

## 911 **Acknowledgments**

912 We thank two anonymous reviewers for their constructive remarks and suggestions.



913 **REFERENCES**

- 914 Abplanalp et al. 2010. An optimised compact electron impact ion storage source for a time-of-  
915 flight mass spectrometer *International Journal of Mass Spectrometry* 294, 33-39.
- 916 Abplanalp, D., Wurz, P., Huber, L., Leya, I., Kopp, E., Rohner, U. Wieser, M., Kalla, L.,  
917 Barabash, S. 2009. A neutral gas mass spectrometer to measure the chemical composition  
918 of the stratosphere *Advances in Space Research*, 44, pp. 870-878
- 919 Aharonson, O., Hayes, A.G., Lunine, J.I., Lorenz, R.D., Allison, M.D., Elachi, C. 2009. An  
920 asymmetric distribution of lakes on Titan as a possible consequence of orbital forcing.  
921 *Nature Geoscience* 2, 851-854.
- 922 Altwegg, K., H. Balsiger, A. Bar-Nun, J.-J. Berthelier, A. Bieler, P. Bochslers, C. Briouis, U.  
923 Calmonte, M. Combi, H. Cottin, J. De Keyser, B. Fiethe, S.A. Fuselier, S. Gasc, T.I.  
924 Gombosi, K.C. Hansen, M. Hässig, A. Jäckel, E. Kopp, A. Korth, L. Le Roy, U. Mall, B.  
925 Marty, O. Mousis, T. Owen, H. Rème, M. Rubin, T. Sémon, C.-Y. Tzou, J.H. Waite, and  
926 P. Wurz, Prebiotic chemicals - amino acid and phosphorus - in the coma of comet  
927 67P/Churyumov-Gerasimenko, *Science Advances* 2:e1600285 (2016) 5pp.
- 928 Artemieva, N., Lunine, J.I. 2005. Impact cratering on Titan II. Global melt, escaping ejecta,  
929 and aqueous alteration of surface organics. *Icarus* 175, 522-533.
- 930 Atreya, S.K., Adams, E.Y., Niemann, H.B., Demick-Montelara, J.E., Owen, T.C.,  
931 Fulchignoni, M., Ferri, F., Wilson, E.H. 2006. Titan's methane cycle. *Planetary and Space*  
932 *Science* 54, 1177-1187.
- 933 Barnes, J.W., Sotin, C., Soderblom, J.M., Brown, R.H., Hayes, A.G., Donelan, M.,  
934 Rodriguez, S., Le Mouélic, S., Baines, K.H. and McCord, T.B., 2014. Cassini/VIMS  
935 observes rough surfaces on Titan's Punga Mare in specular reflection. *Planetary Science*,  
936 3(1), p.1.

- 937 Barnes, J., et al. 2012. AVIATR—Aerial Vehicle for In-Situ and Airborne Titan  
938 Reconnaissance, *Experimental Astronomy*, Vol. 33, No. 1, pp. 55–127.  
939 doi:10.1007/s10686-011-9275-9
- 940 Beghin, C., Randriamboarison, O., Hamelin, M., Karkoschka, E., Sotin, C., Whitten, R.C.,  
941 Berthelier, J.J., Grard, R., Simoes, F. 2012. Analytic theory of Titan's Schumann  
942 resonance: Constraints on ionospheric conductivity and buried water ocean. *Icarus* 218,  
943 1028-1042.
- 944 Behoukova, M., Soucek, O., Hron, J. and Cadek O. 2017. Plume activity and tidal  
945 deformation on Enceladus influenced by faults and variable ice shell thickness,  
946 *Astrobiology*, 17, doi:10.1089/ast.2016.1629.
- 947 Beuthe, M., Rivoldini, A., Trinh, A. 2016. Enceladus's and Dione's floating ice shells  
948 supported by minimum stress isostasy. *Geophysical Research Letters* 43, 10.
- 949 Bèzard, B. 2014. The methane mole fraction in Titan's stratosphere from DISR measurements  
950 during the Huygens probe's descent. *Icarus* 242, 64-73.
- 951 Birch, S.P.D., and 20 colleagues 2017. Geomorphologic mapping of titan's polar terrains:  
952 Constraining surface processes and landscape evolution. *Icarus* 282, 214-236.
- 953 Burr, D.M., Emery, J.P., Lorenz, R.D., Collins, G.C., Carling, P.A. 2006. Sediment transport  
954 by liquid surficial flow: Application to Titan. *Icarus* 181, 235-242.
- 955 Burr, D.M., Drummond, S.A., Cartwright, R., Black, B.A., Perron, J.T. 2013. Morphology of  
956 fluvial networks on Titan: Evidence for structural control. *Icarus* 226, 742-759.
- 957 Čadek, O., and 10 colleagues 2016. Enceladus's internal ocean and ice shell constrained from  
958 Cassini gravity, shape, and libration data. *Geophysical Research Letters* 43, 5653-5660.
- 959 Clark, R.N., Curchin, J.M., Barnes, J.W., Jaumann, R., Soderblom, L., Cruikshank, D.P.,  
960 Brown, R.H., Rodriguez, S., Lunine, J., Stephan, K. and Hoefen, T.M., 2010. Detection

- 961 and mapping of hydrocarbon deposits on Titan. *Journal of Geophysical Research: Planets*,  
962 115(E10).
- 963 Coates, A.J., Crary, F.J., Lewis, G.R., Young, D.T., Waite, J.H., Sittler, E.C. 2007. Discovery  
964 of heavy negative ions in Titan's ionosphere. *Geophysical Research Letters* 34, L22103.
- 965 Coates, A.J., Jones, G.H., Lewis, G.R., Wellbrock, A., Young, D.T., Crary, F.J., Johnson,  
966 R.E., Cassidy, T.A., Hill, T.W. 2010. Negative ions in the Enceladus plume. *Icarus* 206,  
967 618-622.
- 968 Cook-Hallett, C., Barnes, J.W., Kattenhorn, S.A., Hurford, T., Radebaugh, J., Stiles, B.,  
969 Beuthe, M. 2015. Global contraction/expansion and polar lithospheric thinning on Titan  
970 from patterns of tectonism. *Journal of Geophysical Research (Planets)* 120, 1220-1236.
- 971 Cordier, D., Mousis, O., Lunine, J.I., Lebonnois, S., Lavvas, P., Lobo, L.Q., Ferreira, A.G.M.  
972 2010. About the Possible Role of Hydrocarbon Lakes in the Origin of Titan's Noble Gas  
973 Atmospheric Depletion. *The Astrophysical Journal* 721, L117-L120.
- 974 Cornet, T., Cordier, D., Bahers, T.L., Bourgeois, O., Fleurant, C., Mouelic, S.L., Altobelli, N.  
975 2015. Dissolution on Titan and on Earth: Toward the age of Titan's karstic landscapes.  
976 *Journal of Geophysical Research (Planets)* 120, 1044-1074.
- 977 Coustenis, A. and 114 co-authors, TanDEM: Titan and Enceladus Mission, *Experimental*  
978 *Astronomy*, 23, 893-946, 2009
- 979 Coustenis, A., Lunine, J., Lebreton, J.-P., Matson, D., Erd, Ch., Reh, K., Beauchamp, P.,  
980 Lorenz, R., Waite, H., Sotin, Ch., Gurvits, L., Hirtzig, M., 2009. Earth-based support for  
981 the Titan Saturn Mission. *Earth Moon and Planets* 105, 135-142, DOI: 10.1007/s11038-  
982 009-9308-9.
- 983 Coustenis, A., Bampasidis, G., Achterbergh, R. K., Lavvas, P., Nixon, C. A., Jennings, D. E.,  
984 Teanby, N. A., Vinatier, S., Flasar, F. M., Carlson, R. C., Orton, G., Romani, P. N.,

- 985 Guardique, E. A., 2013. Evolution of the stratospheric temperature and chemical  
986 composition over one Titanian year. *Astrophys. J.* 799, 177, 9p.
- 987 Coustenis, A., Jennings, D. E., Achterbergh, R. K., Bampasidis, G., Lavvas, P., Nixon, C. A.,  
988 Teanby, N. A., Anderson, C. M., Flasar, F. M., 2016. Titan's temporal evolution in  
989 stratospheric trace gases near the poles. *Icarus* 270, 409-420.
- 990 Crary, F.J., Magee, B.A., Mandt, K., Waite, J.H., Westlake, J., Young, D.T. 2009. Heavy  
991 ions, temperatures and winds in Titan's ionosphere: Combined Cassini CAPS and INMS  
992 observations. *Planetary and Space Science* 57, 1847-1856.
- 993 Davies, A.G., Sotin, C., Choukroun, M., Matson, D.L., Johnson, T.V. 2016. Cryolava flow  
994 destabilization of crustal methane clathrate hydrate on Titan. *Icarus* 274, 23-32.
- 995 Dougherty, M.K., Khurana, K.K., Neubauer, F.M., Russell, C.T., Saur, J., Leisner, J.S.,  
996 Burton, M.E. 2006. Identification of a Dynamic Atmosphere at Enceladus with the Cassini  
997 Magnetometer. *Science* 311, 1406–1409.
- 998 Dougherty, M.K., Esposito, L.W., Krimigis, S.M. 2009. Saturn from Cassini-Huygens. *Saturn*  
999 *from Cassini-Huygens* .
- 1000 Doyon, R., Hutchings, J., Beaulieu, M., Albert, L., Lafrenière, D., Willott, C., Touahri, D.,  
1001 Rowlands, N., Maszkiewicz, M., Fullerton, A.W. and Volk, K. 2012. The JWST fine  
1002 guidance sensor (FGS) and near-infrared imager and slitless spectrograph (NIRISS). In  
1003 *Proc. SPIE* (Vol. 8442, p. 84422R).
- 1004 Federal Aviation Administration (FAA) Commercial Space Transportation (AST) and the  
1005 Commercial Space Transportation Advisory Committee (COMSTAC) 2015 Commercial  
1006 Space Transportation Forecast April 2015
- 1007 Glein, C.R., Zolotov, M.Y., Shock, E.L. 2008. The oxidation state of hydrothermal systems  
1008 on early Enceladus. *Icarus* 197, 157-163.

- 1009 Glein, C.R., Baross, J.A., Waite, J.H. 2015. The pH of Enceladus' ocean. *Geochimica et*  
1010 *Cosmochimica Acta* 162, 202-219.
- 1011 Goguen, J.D., and 12 colleagues 2013. The temperature and width of an active fissure on  
1012 Enceladus measured with Cassini VIMS during the 14 April 2012 South Pole flyover.  
1013 *Icarus* 226, 1128-1137.
- 1014 Griffith, C.A., Zahnle, K. 1995. Influx of cometary volatiles to planetary moons: The  
1015 atmospheres of 1000 possible Titans. *Journal of Geophysical Research* 100, 16907-16922.
- 1016 Gudipati, M. S., Jacovi, R., Couturier-Tamburelli, I., Lignell, A., Allen, M. 2013.  
1017 Photochemical activity of Titan's low-altitude condensed haze. *Nature Communications*.  
1018 4:1648, DOI: 10.1038/ncomms2649.
- 1019 Hansen, C.J., Esposito, L., Stewart, A.I.F., Colwell, J., Hendrix, A., Pryor, W., Shemansky,  
1020 D., West, R. 2006. Enceladus' Water Vapor Plume. *Science* 311, 1422-1425.
- 1021 Hansen, C.J., Esposito, L.W., Stewart, A.I.F., Meinke, B., Wallis, B., Colwell, J.E., Hendrix,  
1022 A.R., Larsen, K., Pryor, W., Tian, F. 2008. Water vapour jets inside the plume of gas  
1023 leaving Enceladus. *Nature* 456, 477-479.
- 1024 Hansen, C.J., and 10 colleagues 2011. The composition and structure of the Enceladus plume.  
1025 *Geophysical Research Letters* 38, L11202.
- 1026 Hayes, A., and 13 colleagues 2008. Hydrocarbon lakes on Titan: Distribution and interaction  
1027 with a porous regolith. *Geophysical Research Letters* 35, L09204.
- 1028 Hayes, A.G., and 11 colleagues 2010. Bathymetry and absorptivity of Titan's Ontario Lacus.  
1029 *Journal of Geophysical Research (Planets)* 115, E09009.
- 1030 Hayes, A.G., and 14 colleagues 2011. Transient surface liquid in Titan's polar regions from  
1031 Cassini. *Icarus* 211, 655-671.

- 1032 Hedman, M.M., Nicholson, P.D., Showalter, M.R., Brown, R.H., Buratti, B.J., Clark, R.N.  
1033 2009. Spectral Observations of the Enceladus Plume with Cassini-Vims. *The*  
1034 *Astrophysical Journal* 693, 1749-1762.
- 1035 Hofer, L., and 10 colleagues 2015. Prototype of the gas chromatograph-mass spectrometer to  
1036 investigate volatile species in the lunar soil for the Luna-Resurs mission. *Planetary and*  
1037 *Space Science* 111, 126-133.
- 1038 Hörst, S.M., Vuitton, V., Yelle, R.V. 2008. Origin of oxygen species in Titan's atmosphere.  
1039 *Journal of Geophysical Research (Planets)* 113, E10006.
- 1040 Hörst, S.M., and 12 colleagues 2012. Formation of Amino Acids and Nucleotide Bases in a  
1041 Titan Atmosphere Simulation Experiment. *Astrobiology* 12, 809-817.
- 1042 Howett, C.J.A., Spencer, J.R., Pearl, J., Segura, M. 2011. High heat flow from Enceladus'  
1043 south polar region measured using 10-600 cm<sup>-1</sup> Cassini/CIRS data. *Journal of Geophysical*  
1044 *Research (Planets)* 116, E03003.
- 1045 Hsu, H.-W., Postberg, F., Kempf, S., Trieloff, M., Burton, M., Roy, M., Moragas-  
1046 Klostermeyer, G., Srama, R. 2011. Stream particles as the probe of the dust-plasma-  
1047 magnetosphere interaction at Saturn. *Journal of Geophysical Research (Space Physics)*  
1048 116, A09215.
- 1049 Hsu, H.-W., and 14 colleagues 2015. Ongoing hydrothermal activities within Enceladus.  
1050 *Nature* 519, 207-210.
- 1051 Hurford, T.A., Bills, B.G., Helfenstein, P., Greenberg, R., Hoppa, G.V., Hamilton, D.P. 2009.  
1052 Geological implications of a physical libration on Enceladus. *Icarus* 203, 541-552.
- 1053 Iess, L., Rappaport, N.J., Jacobson, R.A., Racioppa, P., Stevenson, D.J., Tortora, P.,  
1054 Armstrong, J.W., Asmar, S.W. 2010. Gravity Field, Shape, and Moment of Inertia of  
1055 Titan. *Science* 327, 1367.

- 1056 Iess, L., Jacobson, R.A., Ducci, M., Stevenson, D.J., Lunine, J.I., Armstrong, J.W., Asmar,  
1057 S.W., Racioppa, P., Rappaport, N.J., Tortora, P. 2012. The Tides of Titan. *Science* 337,  
1058 457.
- 1059 Iess, L., and 10 colleagues 2014. The Gravity Field and Interior Structure of Enceladus.  
1060 *Science* 344, 78-80.
- 1061 Ingersoll, A.P., Pankine, A.A. 2010. Subsurface heat transfer on Enceladus: Conditions under  
1062 which melting occurs. *Icarus* 206, 594-607.
- 1063 Ingersoll, A.P., Ewald, S.P. 2011. Total particulate mass in Enceladus plumes and mass of  
1064 Saturn's E ring inferred from Cassini ISS images. *Icarus* 216, 492-506.
- 1065 Israël, G., and 21 colleagues 2005. Complex organic matter in Titan's atmospheric aerosols  
1066 from in situ pyrolysis and analysis. *Nature* 438, 796-799.
- 1067 Jennings, D.E., Romani, P.N., Bjoraker, G.L., Sada, P.V., Nixon, C.A., Lunsford, A.W.,  
1068 Boyle, R.J., Hesman, B.E., McCabe, G.H. 2009.  $^{12}\text{C}/^{13}\text{C}$  Ratio in Ethane on Titan and  
1069 Implications for Methane's Replenishment. *Journal of Physical Chemistry A* 113, 11101-  
1070 11106.
- 1071 Kite, E.S., Rubin, A.M. 2016. Sustained eruptions on Enceladus explained by turbulent  
1072 dissipation in tiger stripes. *Proceedings of the National Academy of Science* 113, 3972-  
1073 3975.
- 1074 Kliore, A.J., Nagy, A.F., Cravens, T.E., Richard, M.S., Rymer, A.M. 2011. Unusual electron  
1075 density profiles observed by Cassini radio occultations in Titan's ionosphere: Effects of  
1076 enhanced magnetospheric electron precipitation? *Journal of Geophysical Research: Space*  
1077 *Physics*, 116, A11318.
- 1078 Kliore, A.J. et al. 2008. First results from the Cassini radio occultations of the Titan  
1079 ionosphere. *Journal of Geophysical Research: Space Physics* 113 (9), A09317

- 1080 Lammer, H., and 16 colleagues 2009. What makes a planet habitable?. *Astronomy and*  
1081 *Astrophysics Review* 17, 181-249.
- 1082 Lancaster, N. 1989. *The Namib Sand Sea: Dune Forms, Processes, and Sediments*. A.A.  
1083 Balkema, Rotterdam, 200 pp.
- 1084 Leary, J., Jones, C., Lorenz, R., Strain, R. D., and Waite, J. H., Titan Explorer Flagship  
1085 Mission Study, Johns Hopkins Univ., Applied Physics Lab., Laurel, MD, Aug. 2007; also  
1086 [http://www.lpi.usra.edu/opag/Titan\\_Explorer\\_Public\\_Report.pdf](http://www.lpi.usra.edu/opag/Titan_Explorer_Public_Report.pdf), Jan. 2008 [retrieved  
1087 2015].
- 1088 Lemmon, M.T., Karkoschka, E. and Tomasko, M. 1993, Titan's Rotation: Surface Features  
1089 Observed. *Icarus*, 103, pp. 329-332.
- 1090 Liu, Z.Y.C., Radebaugh, J., Harris, R.A., Christiansen, E.H., Neish, C.D., Kirk, R.L., Lorenz,  
1091 R.D. 2016. The tectonics of Titan: Global structural mapping from Cassini RADAR. *Icarus*  
1092 270, 14-29.
- 1093 Loose, M., Beletic, J., Garnett, J. and Muradian, N., 2006, June. Space qualification and  
1094 performance results of the SIDECAR ASIC. In *SPIE Astronomical Telescopes+*  
1095 *Instrumentation* (pp. 62652J-62652J). International Society for Optics and Photonics.
- 1096 Lopes, R.M.C., and 15 colleagues 2007a. The Lakes and Seas of Titan. *EOS Transactions* 88,  
1097 569-570.
- 1098 Lopes, R.M.C., and 43 colleagues 2007b. Cryovolcanic features on Titan's surface as revealed  
1099 by the Cassini Titan Radar Mapper. *Icarus* 186, 395-412.
- 1100 Lopes, R.M.C., and 15 colleagues 2013. Cryovolcanism on Titan: New results from Cassini  
1101 RADAR and VIMS. *Journal of Geophysical Research (Planets)* 118, 416-435.
- 1102 Lopes, R.M.C., Malaska, M.J., Solomonidou, A., LeGall, A., Janssen, M.A., Neish, C.,  
1103 Turtle, E.P., Birch, S.P.D., Hayes, A.G., Radebaugh, J., Coustenis, A., Schoenfeld, A.,  
1104 Stiles, B.W., Kirk, R.L., Mitchell, K.L., Stofan, E.R., Lawrence, K.J., and the Cassini



- 1105 RADAR Team 2016. Nature, Distribution, and Origin of Titan's Undifferentiated Plains  
1106 ("Blandlands"). *Icarus*, 270, 162-182.
- 1107 Lorenz, R.D., and 39 colleagues 2006. The Sand Seas of Titan: Cassini RADAR Observations  
1108 of Longitudinal Dunes. *Science* 312, 724-727.
- 1109 Lorenz, R. D. 2000. Post-Cassini Exploration of Titan: Science Rationale and Mission  
1110 Concepts, *Journal of the British Interplanetary Society*, Vol. 53, pp. 218–234.
- 1111 Lorenz, R. D. 2009. A Review of Titan Mission Studies, *Journal of the British Interplanetary*  
1112 *Society*, 62, 162-174.
- 1113 Lunine, J.I. 2017. Ocean worlds exploration. *Acta Astronautica* 131, 123-130.
- 1114 Maciaszek, T., Ealet, A., Jahnke, K., Prieto, E., Barbier, R., Mellier, Y., Costille, A., Ducret,  
1115 F., Fabron, C., Gimenez, J.L. and Grange, R., 2014, August. Euclid near infrared  
1116 spectrophotometer instrument concept and first test results at the end of phase B. In *SPIE*  
1117 *Astronomical Telescopes+ Instrumentation* (pp. 91430K-91430K). International Society  
1118 for Optics and Photonics.
- 1119 MacKenzie, S.M., and 10 colleagues 2014. Evidence of Titan's climate history from evaporite  
1120 distribution. *Icarus* 243, 191-207.
- 1121 Malaska, M.J., Lopes, R.M., Hayes, A.G., Radebaugh, J., Lorenz, R.D., Turtle, E.P. 2016.  
1122 Material transport map of Titan: The fate of dunes. *Icarus* 270, 183-196.
- 1123 Mandt, K.E., and 18 colleagues 2012. Ion densities and composition of Titan's upper  
1124 atmosphere derived from the Cassini Ion Neutral Mass Spectrometer: Analysis methods  
1125 and comparison of measured ion densities to photochemical model simulations. *Journal of*  
1126 *Geophysical Research (Planets)* 117, E10006.
- 1127 McKay, C.P., Porco, C., Altheide, T., Davis, W.L., Kral, T.A. 2008. The Possible Origin and  
1128 Persistence of Life on Enceladus and Detection of Biomarkers in the Plume. *Astrobiology*  
1129 8, 909-919.

- 1130 McKay, C.P. 2016. Titan as the Abode of Life. *Life*, 6, 8.
- 1131 McKinnon, W.B. 2015. Effect of Enceladus's rapid synchronous spin on interpretation of  
1132 Cassini gravity. *Geophysical Research Letters* 42, 2137-2143.
- 1133 Mitri, G., Showman, A.P., Lunine, J.I., Lorenz, R.D. 2007. Hydrocarbon lakes on Titan.  
1134 *Icarus* 186, 385-394.
- 1135 Mitri, G., Bland, M.T., Showman, A.P., Radebaugh, J., Stiles, B., Lopes, R.M.C., Lunine, J.I.,  
1136 Pappalardo, R.T. 2010. Mountains on Titan: Modeling and observations. *Journal of*  
1137 *Geophysical Research (Planets)* 115, E10002.
- 1138 Mitri, G., and 16 colleagues 2014a. The exploration of Titan with an orbiter and a lake probe.  
1139 *Planetary and Space Science* 104, 78-92.
- 1140 Mitri, G., Meriggiola, R., Hayes, A., Lefevre, A., Tobie, G., Genova, A., Lunine, J.I., Zebker,  
1141 H. 2014b. Shape, topography, gravity anomalies and tidal deformation of Titan. *Icarus*  
1142 236, 169-177.
- 1143 Moore, J.M., Howard, A.D. 2010. Are the basins of Titan's Hotei Regio and Tui Regio sites  
1144 of former low latitude seas?. *Geophysical Research Letters* 37, L22205.
- 1145 Mousis, O., Schmitt, B. 2008. Sequestration of Ethane in the Cryovolcanic Subsurface of  
1146 Titan. *The Astrophysical Journal* 677, L67.
- 1147 Mousis, O., and 10 colleagues 2009. Clathration of Volatiles in the Solar Nebula and  
1148 Implications for the Origin of Titan's Atmosphere. *The Astrophysical Journal* 691, 1780-  
1149 1786.
- 1150 Mousis, O., Lunine, J.I., Picaud, S., Cordier, D., Waite, J.H., Jr., Mandt, K.E. 2011. Removal  
1151 of Titan's Atmospheric Noble Gases by Their Sequestration in Surface Clathrates. *The*  
1152 *Astrophysical Journal* 740, L9.
- 1153 Neish, C.D., Lorenz, R.D. 2012. Titan's global crater population: A new assessment.  
1154 *Planetary and Space Science* 60, 26-33.

- 1155 Neish, C.D., and 14 colleagues 2015. Spectral properties of Titan's impact craters imply  
1156 chemical weathering of its surface. *Geophysical Research Letters* 42, 3746-3754.
- 1157 Neish, C.D., Molaro, J.L., Lora, J.M., Howard, A.D., Kirk, R.L., Schenk, P., Bray, V.J.,  
1158 Lorenz, R.D. 2016. Fluvial erosion as a mechanism for crater modification on Titan. *Icarus*  
1159 270, 114-129.
- 1160 Niemann, H.B., and 17 colleagues 2005. The abundances of constituents of Titan's  
1161 atmosphere from the GCMS instrument on the Huygens probe. *Nature* 438, 779-784.
- 1162 Niemann, H.B., Atreya, S.K., Demick, J.E., Gautier, D., Haberman, J.A., Harpold, D.N.,  
1163 Kasprzak, W.T., Lunine, J.I., Owen, T.C., Raulin, F. 2010. Composition of Titan's lower  
1164 atmosphere and simple surface volatiles as measured by the Cassini-Huygens probe gas  
1165 chromatograph mass spectrometer experiment. *Journal of Geophysical Research (Planets)*  
1166 115, E12006.
- 1167 Nimmo, F., Pappalardo, R.T. 2016. Ocean worlds in the outer solar system, *J. Geophys. Res.*,  
1168 121,1378-1399.
- 1169 Nixon, C.A., and 12 colleagues 2012. Isotopic Ratios in Titan's Methane: Measurements and  
1170 Modeling. *The Astrophysical Journal* 749, 159.
- 1171 Owen, T., Niemann, H.B. 2009. The origin of Titan's atmosphere: some recent advances.  
1172 *Philosophical Transactions of the Royal Society of London Series A* 367, 607-615.
- 1173 Porco, C.C., and 24 colleagues 2006. Cassini Observes the Active South Pole of Enceladus.  
1174 *Science* 311, 1393-1401.
- 1175 Porco, C., DiNino, D., Nimmo, F. 2014. How the Geysers, Tidal Stresses, and Thermal  
1176 Emission across the South Polar Terrain of Enceladus are Related. *The Astronomical*  
1177 *Journal* 148, 45.

- 1178 Postberg, F., Kempf, S., Hillier, J.K., Srama, R., Green, S.F., McBride, N., Grun, E. 2008.  
1179 The E-ring in the vicinity of Enceladus. II. Probing the moon's interior. The composition of  
1180 E-ring particles. *Icarus* 193, 438-454.
- 1181 Postberg, F., Kempf, S., Rost, D., Stephan, T., Srama, R., Trieloff, M., Mocker, A., Goerlich,  
1182 M. 2009. Discriminating contamination from particle components in spectra of Cassini's  
1183 dust detector CDA. *Planetary and Space Science* 57, 1359-1374.
- 1184 Postberg, F., Kempf, S., Schmidt, J., Brilliantov, N., Beinsen, A., Abel, B., Buck, U., Srama,  
1185 R. 2009. Sodium salts in E-ring ice grains from an ocean below the surface of Enceladus.  
1186 *Nature* 459, 1098-1101.
- 1187 Postberg, F., Schmidt, J., Hillier, J., Kempf, S., Srama, R. 2011. A salt-water reservoir as the  
1188 source of a compositionally stratified plume on Enceladus. *Nature* 474, 620-622.
- 1189 Postberg, F., Khawaja, N., Hsu, H.W., Sekine, Y., Shibuya, T. 2015. Refractory Organic  
1190 Compounds in Enceladus' Ice Grains and Hydrothermal Activity. AGU Fall Meeting  
1191 Abstracts.
- 1192 Radebaugh, J., Lorenz, R.D., Kirk, R.L., Lunine, J.I., Stofan, E.R., Lopes, R.M.C., Wall,  
1193 S.D., the Cassini Radar Team 2007. Mountains on Titan observed by Cassini Radar. *Icarus*  
1194 192, 77-91.
- 1195 Radebaugh, J., and 15 colleagues 2008. Dunes on Titan observed by Cassini Radar. *Icarus*  
1196 194, 690-703.
- 1197 Rappaport, N.J., Iess, L., Wahr, J., Lunine, J.I., Armstrong, J.W., Asmar, S.W., Tortora, P., Di  
1198 Benedetto, M., Racioppa, P., 2008. Can Cassini detect a subsurface ocean in Titan from  
1199 gravity measurements? *Icarus* 194, 711–720.
- 1200 Rauscher, B.J., Figer, D.F., Regan, M.W., Boeker, T., Garnett, J., Hill, R.J., Bagnasco, G.,  
1201 Balleza, J., Barney, R., Bergeron, L.E. and Brambora, C., 2004, October. Detectors for the  
1202 James Webb Space Telescope near-infrared spectrograph. In *SPIE Astronomical*

- 1203 Telescopes+ Instrumentation (pp. 710-726). International Society for Optics and  
1204 Photonics.
- 1205 Reh, K., Spilker, L., Lunine, J.I., Waite, J.H., Cable, M.L., Postberg, F. and Clark, K., 2016,  
1206 March. Enceladus Life Finder: The search for life in a habitable Moon. In Aerospace  
1207 Conference, 2016 IEEE (pp. 1-8)
- 1208 Rieke, M.J., Kelly, D. and Horner, S., 2005, August. Overview of James Webb Space  
1209 Telescope and NIRCams Role. In Optics & Photonics 2005 (pp. 590401-590401).  
1210 International Society for Optics and Photonics.
- 1211 Roth, L., Saur, J., Retherford, K.D., Strobel, D.F., Feldman, P.D., McGrath, M.A., Nimmo, F.  
1212 2014. Transient Water Vapor at Europa's South Pole. *Science* 343, 171-174.
- 1213 Scherer, S., K. Altwegg, H. Balsiger, J. Fischer, A. Jäckel, A. Korth, M. Mildner, D. Piazza,  
1214 H. Rème, and P. Wurz, A novel principle for an ion mirror design in time-of-flight mass  
1215 spectrometry, *Int. Jou. Mass Spectr.* 251 (2006) 73–81.
- 1216 Schinder, P.J. et al. 2015. A numerical technique for two-way radio occultations by oblate  
1217 axisymmetric atmospheres with zonal winds. *Radio Science* 50 (7), pp. 712-727.
- 1218 Schinder, P.J. et al. 2012. The structure of Titan's atmosphere from Cassini radio occultations:  
1219 Occultations from the Prime and Equinox missions. *Icarus*, 221, 1020-1031.
- 1220 Schmidt, J., Brilliantov, N., Spahn, F., Kempf, S. 2008. Slow dust in Enceladus' plume from  
1221 condensation and wall collisions in tiger stripe fractures. *Nature* 451, 685-688.
- 1222 Schubert, G., Anderson, J.D., Travis, B.J., Palguta, J. 2007. Enceladus: Present internal  
1223 structure and differentiation by early and long-term radiogenic heating. *Icarus* 188, 345-  
1224 355.
- 1225 Senft, L.E., Stewart, S.T. 2011. Modeling the morphological diversity of impact craters on icy  
1226 satellites. *Icarus* 214, 67-81.

- 1227 Serigano, J., Nixon, C.A., Cordiner, M.A., Irwin, P.G.J., Teanby, N.A., Charnley, S.B.,  
1228 Lindberg, J.E. 2016. Isotopic Ratios of Carbon and Oxygen in Titan's CO using ALMA.  
1229 The Astrophysical Journal 821, L8.
- 1230 Soderblom, J.M., Brown, R.H., Soderblom, L.A., Barnes, J.W., Jaumann, R., Le Mouélic, S.,  
1231 Sotin, C., Stephan, K., Baines, K.H. and Buratti, B.J., Clark, R.N., Nicholson, P.D., 2010.  
1232 Geology of the Selk crater region on Titan from Cassini VIMS observations. Icarus,  
1233 208(2), pp.905-912.
- 1234 Soderblom, J.M., Barnes, J.W., Soderblom, L.A., Brown, R.H., Griffith, C.A., Nicholson,  
1235 P.D., Stephan, K., Jaumann, R., Sotin, C., Baines, K.H. and Buratti, B.J., 2012. Modeling  
1236 specular reflections from hydrocarbon lakes on Titan. Icarus, 220(2), pp.744-751.
- 1237 Soderblom, L.A., Becker, T.L., Kieffer, S.W., Brown, R.H., Hansen, C.J., Johnson, T.V.,  
1238 Kirk, R.L., Shoemaker, E.M., Cook, A.F. 1990. Triton's geyser-like plumes - Discovery  
1239 and basic characterization. Science 250, 410-415.
- 1240 Soderblom, L.A., and 26 colleagues 2007. Correlations between Cassini VIMS spectra and  
1241 RADAR SAR images: Implications for Titan's surface composition and the character of  
1242 the Huygens Probe Landing Site. Planetary and Space Science 55, 2025-2036.
- 1243 Solomonidou, A., Hirtzig, M., Coustenis, A., Bratsolis, E., Le Mouélic, S., Rodriguez, S.,  
1244 Stephan, K., Drossart, P., Sotin, C., Jaumann, R., Brown, R.H., Kyriakopoulos, K., Lopes,  
1245 R.M.C., Bampasidis, G., Stamatelopoulou-Seymour, K., Moussas, X. (2014). Surface  
1246 albedo spectral properties of geologically interesting areas on Titan. J. of Geophys. Res.,  
1247 119, 1729-1747.
- 1248 Solomonidou, A., Coustenis, M., Hirtzig, S., Rodriguez, K., Stephan, R.M.C. Lopes, P.  
1249 Drossart, C. Sotin, S. Le Mouélic, K. Lawrence, E. Bratsolis, R. Jaumann and R.H. Brown,  
1250 (2016). Temporal variations of Titan's surface with Cassini/VIMS, Icarus 270, 85-99.

- 1251 Sotin, C. et al., 2005. Release of volatiles from a possible cryovolcano from near-infrared  
1252 imaging of Titan. *Nature*, 435, 786-798.
- 1253 Sotin, C., Mitri, G., Rappaport, N., Schubert, G., Stevenson, D. 2010. Titan's Interior  
1254 Structure. *Titan from Cassini-Huygens* 61.
- 1255 Spahn, F., and 15 colleagues 2006. Cassini Dust Measurements at Enceladus and Implications  
1256 for the Origin of the E Ring. *Science* 311, 1416-1418.
- 1257 Sparks, W. B., Hand, K. P. , McGrath, M. A., Bergeron, E., Cracraft, M., and Deustua, S. E.,  
1258 2016. Probing for Evidence of Plumes on Europa with HST/STIS. *Ap. J.* 829:121.
- 1259 Sparks, W.B., Schmidt, McGrath, M. A., Hand, K. P., Spencer, J. R., Cracraft, M., and  
1260 Deustua, S. E, 2017. Active Cryovolcanism on Europa?, *Ap. J. Lett.*, 839:L18.
- 1261 Srama, R., and 43 colleagues 2004. The Cassini Cosmic Dust Analyzer. *Space Science*  
1262 *Reviews* 114, 465–518
- 1263 Srama, R., and 17 colleagues 2015. Enceladus Icy Jet Analyzer (ENIJA): Search for life with  
1264 a high resolution TOF-MS for in situ characterization of high dust density regions.  
1265 *European Planetary Science Congress 2015*, EPSC2015-769.
- 1266 Stofan, E.R., and 37 colleagues 2007. The lakes of Titan. *Nature* 445, 61-64.
- 1267 Stofan, E., Lorenz, R., Lunine, J., Bierhaus, E., Clark, B., Mahaffy, P., and Ravine, M.,  
1268 TiME—The Titan Mare Explorer, *IEEE Aerospace Conference*, IEEE Publ., Piscataway,  
1269 NJ, March 2013, pp. 1–10.
- 1270 Strange, N., Spilker, T., Landau, D., Lam, T., Lyons, D. and Guzman, J., 2009. Mission  
1271 Design for the Titan Saturn System Mission Concept. *Advances in the Astronautical*  
1272 *Sciences*, 135(2), pp.919-934.
- 1273 Thomas, P.C., Tajeddine, R., Tiscareno, M.S., Burns, J.A., Joseph, J., Lored, T.J.,  
1274 Helfenstein, P., Porco, C. 2016. Enceladus's measured physical libration requires a global  
1275 subsurface ocean. *Icarus* 264, 37-47.

- 1276 Thompson, W.R., Sagan, C. 1992. Organic chemistry on Titan: Surface interactions.  
1277 Symposium on Titan 338.
- 1278 Tobie, G., Teanby, N.A., Coustenis, A., Jaumann, R., Raulin, F., Schmidt, J., Carrasco, N.,  
1279 Coates, A.J., Cordier, D., De Kok, R. and Geppert, W.D., 2014. Science goals and mission  
1280 concept for the future exploration of Titan and Enceladus. *Planetary and Space Science*,  
1281 104, pp.59-77.
- 1282 Tobie, G., Lunine, J.I., Sotin, C. 2006. Episodic outgassing as the origin of atmospheric  
1283 methane on Titan. *Nature* 440, 61-64.
- 1284 Tobie, G., Gautier, D., Hersant, F. 2012. Titan's Bulk Composition Constrained by Cassini-  
1285 Huygens: Implication for Internal Outgassing. *The Astrophysical Journal* 752, 125.
- 1286 Tomasko, M.G., and 39 colleagues 2005. Rain, winds and haze during the Huygens probe's  
1287 descent to Titan's surface. *Nature* 438, 765-778.
- 1288 Tortora, P., Zannoni, M., Hemingway, D., Nimmo, F., Jacobson, R.A., Iess, L., Parisi, M.  
1289 2016. Rhea gravity field and interior modeling from Cassini data analysis. *Icarus* 264, 264-  
1290 273.
- 1291 Turtle, E.P., and 13 colleagues 2011. Rapid and Extensive Surface Changes Near Titan's  
1292 Equator: Evidence of April Showers. *Science* 331, 1414.
- 1293 Vuitton, V., Yelle, R.V., McEwan, M.J. 2007. Ion chemistry and N-containing molecules in  
1294 Titan's upper atmosphere. *Icarus* 191, 722-742.
- 1295 Yelle, R.V., Cui, J., Müller-Wodarg, I.C.F. 2008. Methane escape from Titan's atmosphere.  
1296 *Journal of Geophysical Research (Planets)* 113, E10003.
- 1297 Yung, Y.L., Allen, M., Pinto, J.P. 1984. Photochemistry of the atmosphere of Titan -  
1298 Comparison between model and observations. *The Astrophysical Journal Supplement*  
1299 *Series* 55, 465-506.



- 1300 Waite, J.H., and 13 colleagues 2006. Cassini Ion and Neutral Mass Spectrometer: Enceladus  
1301 Plume Composition and Structure. *Science* 311, 1419-1422.
- 1302 Waite, J.H., Young, D.T., Cravens, T.E., Coates, A.J., Crary, F.J., Magee, B., Westlake, J.  
1303 2007. The Process of Tholin Formation in Titan's Upper Atmosphere. *Science* 316, 870.
- 1304 Waite, J.H., Jr., and 15 colleagues 2009. Liquid water on Enceladus from observations of  
1305 ammonia and  $^{40}\text{Ar}$  in the plume. *Nature* 460, 487-490.
- 1306 Waite, J. H. et al. 2006. Cassini ion and neutral mass spectrometer: Enceladus plume  
1307 composition and structure. *Science*, 311(5766), 1419-1422.
- 1308 Waite, J.H., and 12 colleagues 2017. Cassini finds molecular hydrogen in the Enceladus  
1309 plume: Evidence for hydrothermal processes. *Science*, 356 (6334), 155-159.
- 1310 Wilson, E.H., Atreya, S.K. 2009. Titan's Carbon Budget and the Case of the Missing Ethane.  
1311 *Journal of Physical Chemistry A* 113, 11221-11226.
- 1312 Wurz, P., Abplanalp, D., Tulej, M., Lammer, H. 2012. A neutral gas mass spectrometer for  
1313 the investigation of lunar volatiles. *Planetary and Space Science* 74, 264-269.
- 1314 Wurz, P., and 18 colleagues 2015. Solar wind sputtering of dust on the surface of 67P  
1315 Churyumov-Gerasimenko. *Astronomy and Astrophysics* 583, A22.
- 1316 Zahnle, K., Pollack, J.B., Grinspoon, D., Dones, L. 1992. Impact-generated atmospheres over  
1317 Titan, Ganymede, and Callisto. *Icarus* 95, 1-23.
- 1318 Zahnle, K.J., Korycansky, D.G., Nixon, C.A. 2014. Transient climate effects of large impacts  
1319 on Titan. *Icarus* 229, 378-391.

ACCEPTED MANUSCRIPT



<p><b>A.2: What is the history and extent of volatile exchange on Titan?</b></p>	Do Enceladus' volatile compounds originate from a unique reservoir and, if so, how is their distribution between solid and vapour phases affected by eruption processes?	Determine the compositional profile of major species through the plume (both volatile and non-volatile) from mass spectra of plume vapour and condensed phases in icy grains	INMS	Dynamic range Resolution Sensitivity	6/8 decades 300 m/Δm 10 <sup>3</sup> #/cm <sup>3</sup>	6/10 decades 5000 m/Δm 10 <sup>0</sup> #/cm <sup>3</sup>
	How were Titan's volatiles delivered, and were they internally processed?	Quantify the abundance of noble gases in the atmosphere	INMS	Dynamic range Resolution	6/8 decades 3000–5000 m/Δm	6/10 decades 5000 m/Δm
		Measure and compare isotopic ratios: <sup>12</sup> C/ <sup>13</sup> C and D/H in the atmospheric main constituents	INMS	Dynamic range Resolution Sensitivity	6 decades 3000 m/Δm 10 <sup>5</sup> #/cm <sup>3</sup>	6 decades 5000 m/Δm 10 <sup>0</sup> #/cm <sup>3</sup>
	What is the age of Titan's methane cycle, and is there evidence for renewal from internal outgassing?	Measure and compare isotopic ratios: ( <sup>14</sup> N/ <sup>15</sup> N; <sup>12</sup> C/ <sup>13</sup> C; D/H; <sup>16</sup> O/ <sup>18</sup> O) in the upper atmosphere	INMS	Dynamic range Resolution Sensitivity	6/8 decades 3000 m/Δm 10 <sup>3</sup> #/cm <sup>3</sup>	6/10 decades 5000 m/Δm 10 <sup>0</sup> #/cm <sup>3</sup>
		Constrain the genesis of candidate cryovolcanoes and cryovolcanic flows	TIGER	Coverage Scale Wavelength DTM vertical resol.	Sotra, Tui, & Hotei 50 m/pixel 3 colours 20 m	Sotra, Tui, & Hotei 30–50 m/pixel 3 colours 15–20 m
		Determine whether seas have existed in the tropics and/or south polar region	TIGER	Coverage	Regions within Hotei, Tui, Xanadu & the putative south- polar basins 100m/pix 3 colour N/A	Regions within Hotei, Tui, Xanadu & the putative south- polar basins 100m/pix 3 colour N/A
	How does Titan's surface reflect climate change?	Investigate fine-scale dune patterns and how they reorient or breakup	TIGER	Coverage Scale Wavelength DTM vertical resol.	4 dune regions 50m/pix 3 colour N/A	4 dune regions 30–50m/pix 3 colour N/A

<p><b>A.3: How has Titan's organic-rich surface evolved?</b></p>	<p>How have liquid organics modified Titan's surface?</p>	<p>Investigate the morphology of river networks and channels</p>	TIGER	<p>Coverage Scale Wavelength DTM vertical resol.</p>	<p>3 drainages 30m/pix 3 colour 15 m</p>	<p>3 drainages 25–30m/pix 3 colour 10–15 m</p>
		<p>Determine whether the labyrinth terrains and sharp edged depressions are formed by dissolution</p>	TIGER	<p>Coverage Scale Wavelength DTM vertical resol.</p>	<p>2 regions 100m/pix 3 colour 40 m</p>	<p>2 regions 50–100m/pix 3 colour 20–40 m</p>
	<p>To what degree are sediments produced and transported by fluvial and eolian processes?</p>	<p>Investigate the margins of the dune fields to identify sources and sinks of sand</p>	TIGER	<p>Coverage Scale Wavelength DTM vertical resol.</p>	<p>4 dune regions 50m/pix 3 colour N/A</p>	<p>4 dune regions 30–50m/pix 3 colour N/A</p>
		<p>Determine the primary erosion processes that degrade impact crater rims</p>	TIGER	<p>Coverage Scale Wavelength DTM vertical resol.</p>	<p>4 impacts 100m/pix 3 colour N/A</p>	<p>4 impacts 50–100m/pix 3 colour N/A</p>
	<p>How do the mechanical and chemical properties (i.e., composition) vary between the observed geologic units on Titan?</p>	<p>Investigate the fine-scale geologic processes that modify the plains</p>	TIGER	<p>Coverage Scale Wavelength DTM vertical resol.</p>	<p>3 regions 50m/pix 3 colour N/A</p>	<p>3 regions 30–50m/pix 3 colour N/A</p>
		<p>Determine how fluvial erosion varies among geologic units</p>	TIGER	<p>Coverage Scale Wavelength DTM vertical resol.</p>	<p>5 regions 50m/pix 3 colour N/A</p>	<p>5 regions 30–50m/pix 3 colour N/A</p>
		<p>Constrain the maximum slopes and topography supported by different geologic units</p>	TIGER	<p>Coverage Scale Wavelength DTM vertical resol.</p>	<p>5 regions 100m/pix 3 colour 40m</p>	<p>5 regions 50–100m/pix 3 colour 20–40m</p>
		<p>Investigate the morphology, topography, and spectral relationships across unit boundaries</p>	TIGER	<p>Coverage Scale Wavelength DTM vertical resol.</p>	<p>5 boundaries 100m/pix 3 colour 40m</p>	<p>5 boundaries 50–100m/pix 3 colour 20–40m</p>

GOAL B: HABITABILITY AND POTENTIAL FOR LIFE IN OCEAN WORLDS, ENCELADUS AND TITAN						
Science Objectives	Scientific Questions	Measurement Description	Instrument	Measurement Requirements		
				Parameter	Requirement	Performance
<b>B.1: Is Enceladus' aqueous interior an environment favourable to the emergence of life?</b>	What is the nature of hydrothermal activity on Enceladus and how does it connect with the plume activity?	Detect and inventory reduced and oxidized species in the plume material (e.g., $\text{NH}_3/\text{N}_2$ ratio, $\text{H}_2$ abundance, reduced versus oxidized organic species)	INMS	Dynamic range Resolution Sensitivity	6/8 decades 3000m/ $\Delta$ m $10^3$ #/cm <sup>3</sup>	6/10 decades 5000m/ $\Delta$ m $10^0$ #/cm <sup>3</sup>
			ENIJA	Dynamic range Mass range Resolution Sensitivity	4 decades 7–200 m/z 200 m/ $\Delta$ m 1 ppm	6/8 decades 1–2000m/z 1000m/ $\Delta$ m 0.1 ppm
		ENIJA	Characterize composition and abundance of salts and other minerals as messengers of rock/water interaction from mass spectra of icy grains	Dynamic range Mass range Resolution Sensitivity	6 decades 7–200 m/z 200 m/ $\Delta$ m 1 ppm	6/8 decades 1–2000m/z 1000m/ $\Delta$ m 0.1 ppm
		ENIJA	Determine spatial variations in plume composition (vapour and icy grains) and correlate with source activity	Dynamic range Mass resolution Resolution Sensitivity Spatial Resolution	4 decades 7–500 m/z 500 m/ $\Delta$ m 1 ppm 1000 m	6/8 decades 1–2000m/z 1000m/ $\Delta$ m 0.1 ppm 100 m
		TIGER		Coverage Scale Wavelength DTM vertical res.	2 cross-stripe tracks 5m/pix 5 & 5.3 $\mu$ m N/A	2 cross-stripe tracks 2.5–5m/pix 5 & 5.3 $\mu$ m N/A
		TIGER	Determine how much energy the jets dissipate	Coverage Scale Wavelength DTM vertical res.	2 night-time cross-stripe tracks 5m/pix 5 & 5.3 $\mu$ m N/A	2 cross-stripe tracks 2.5–5m/pix 5 & 5.3 $\mu$ m N/A

			Compare mass distribution of organic molecules to that expected from abiotic synthesis (e.g., Poisson versus non-Poisson) in the mass distribution of organic molecules	INMS	Dynamic range Resolution Sensitivity	6/10 decades 5000m/Δm 10 <sup>0</sup> #/cm <sup>3</sup>
			Search for abnormal isotopic ratio in organics in plume vapour, including allowing the separation of species with isobaric interferences for example, <sup>12</sup> CH from <sup>13</sup> C	ENJA	Dynamic range Mass range Resolution Sensitivity	6/8 decades 3000m/Δm 10 <sup>3</sup> #/cm <sup>3</sup>
			Search for amino acids and abnormal <sup>12</sup> C/ <sup>13</sup> C ratio in organics that may have been captured in the ice matrix of solid plume material	INMS	Dynamic range Resolution Sensitivity	6/8 decades 5000 m/Δm 10 <sup>0</sup> #/cm <sup>3</sup>
			Search for amino acids and abnormal <sup>12</sup> C/ <sup>13</sup> C ratio in organics that may have been captured in the ice matrix of solid plume material	ENJA	Dynamic range Mass range Resolution Sensitivity	6/8 decades 1-2000m/z 1000m/Δm 0.1 ppm
			Measure the elemental chemistry of low mass organic molecules in Titan's atmosphere	INMS	Dynamic range Resolution Sensitivity	6/10 decades 5000m/Δm 10 <sup>0</sup> #/cm <sup>3</sup>
			Measure organic macromolecules and ionic species (cations and anions) in order to monitor chemical coupling processes between ions and neutral species	INMS	Dynamic range Resolution Sensitivity	6/10 decades 5000m/Δm 10 <sup>0</sup> #/cm <sup>3</sup>
			Characterize the structure of haze layers, along with their spatial and temporal variations	TIGER	Coverage Scale	10 temporally spaced full-disk images 500m-1km/pix
		Is there evidence that biotic/prebiotic processes are operating in Enceladus' interior?				
<b>B.2: To what level of complexity has prebiotic chemistry evolved in the Titan system?</b>		What chemical processes control the formation and evolution of complex organics in Titan's atmosphere?				

					Wavelength DTM vertical resol.	3 colours N/A	3 colours N/A
	Determine the cloud distribution and morphology, including estimates of their top altitudes and vertical extent	TIGER			Coverage  Scale Wavelength DTM vertical resol.	10 temporally spaced full-disk images 1km/pix 3 colours N/A	10 temporally spaced full-disk images 500m–1km/pix 3 colours N/A
	Investigate the morphology and compositional variability of candidate cryovolcanoes	TIGER			Coverage  Scale Wavelength DTM vertical resol.	Sotra, Tui & Hotei 50m/pix 3 colours 20m	Sotra, Tui & Hotei 30–50m/pix 3 colours 15–20m
	Investigate the morphology of Titan's mountains to look for evidence of compressional vs extensional tectonics	TIGER			Coverage Scale Wavelength DTM vertical resol.	3 mountains 100 m/pix 3 colours 40 m	3 mountains 50–100 m/pix 3 colours 20–40 m
	Investigate melt sheets and flows associated with impact craters	TIGER			Coverage  Scale Wavelength DTM vertical resol.	2 larger fresh craters 50 m/pix 3 colours N/A	2 larger fresh craters 30–50 m/pix 3 colours N/A
	Measure the abundance of radiogenically derived noble gases (e.g., <sup>40</sup> Ar, <sup>21</sup> Ne) and helium	INMS			Dynamic range Resolution Sensitivity	6/8 decades 3000m/Δm 10 <sup>1</sup> #/cm <sup>3</sup>	6/10 decades 5000m/Δm 10 <sup>0</sup> #/cm <sup>3</sup>
	To what extent does Titan's organic-rich surface chemically communicate with its water-rich interior?						



76 **Table 2.** Summary of Instrument Characteristics.

Instrument/ Experiment (Proposed Agency)	Mass (kg)	Peak Power (W)	TRL	Science Contribution
INMS (SSO)	6.2	34	6	1) Analysis of elemental, molecular and isotopic composition of neutral and ionic gas phase constituents in a mass-to-charge range of 1–1000 u in Saturn’s E-ring, Enceladus’ plume and Titan’s upper atmosphere 2) Search for spatial variations in composition and correlate with jet sources.
ENIJA (DLR)	6.5	19.2	5–6	1) Analysis of elemental, molecular and isotopic composition of solid phase constituents in a mass-to-charge range of 1–2000 u of Enceladus’ plume / E-ring 2) Measure fluxes at high impact rates up to $108 \text{ s}^{-1}\text{m}^{-2}$ to map the dynamical profile (number density, ejection speeds and size distribution) of Enceladus’ ice jets
TIGER (NASA)	45	30	5–6	1) Detailed analysis of the geology of Titan’s surface at 30–100 m/pixel and of Enceladus’ plume sources at 1 m/pixel 2) Measure of the thermal emission from Enceladus’s south polar terrain, at 1 m/pixel
Total	57.7	83.2		

77

78

79

80 **Table 3.** Nominal interplanetary trajectory

<b>Departure</b>	
Launch date to GTO	April 2030
Hyperbolic Injection date	27 April 2030
Injection $\Delta V$ from upper stage (km/s)	1.20
Injected Mass (kg)	4056
$C_3$ ( $\text{km}^2/\text{s}^2$ )	9.58
Declination of escape asymptote (deg)	5
<b>Cruise</b>	
Earth flyby date	20 August 2031
Earth flyby altitude (km)	500
Earth flyby V-infinity (km/s)	9.28
S/C mass at Earth flyby	3637
<b>Arrival</b>	
Saturn arrival date	26 April 2036
Flight time (years)	6.0
Arrival V-infinity (km/s)	5.72
Arrival declination (deg)	19.0
SOI $\Delta V$ (m/s)	569
Range at SOI ( $R_S$ )	1.05
Orbital period (day)	150
Apoapsis range ( $R_S$ )	180
S/C mass after SOI (kg)	2753

81

82

83 **Table 4.** Launch period performance, fixed arrival date.

Launch Date	Nominal -10 days	Nominal (27Apr2030)	Nominal+10days
$C_3$ (km <sup>2</sup> /s <sup>2</sup> )	9.58	9.58	9.58
Xe propellant (kg)	750	747	752
SOI $\Delta V$ (m/s)	563	569	571

84

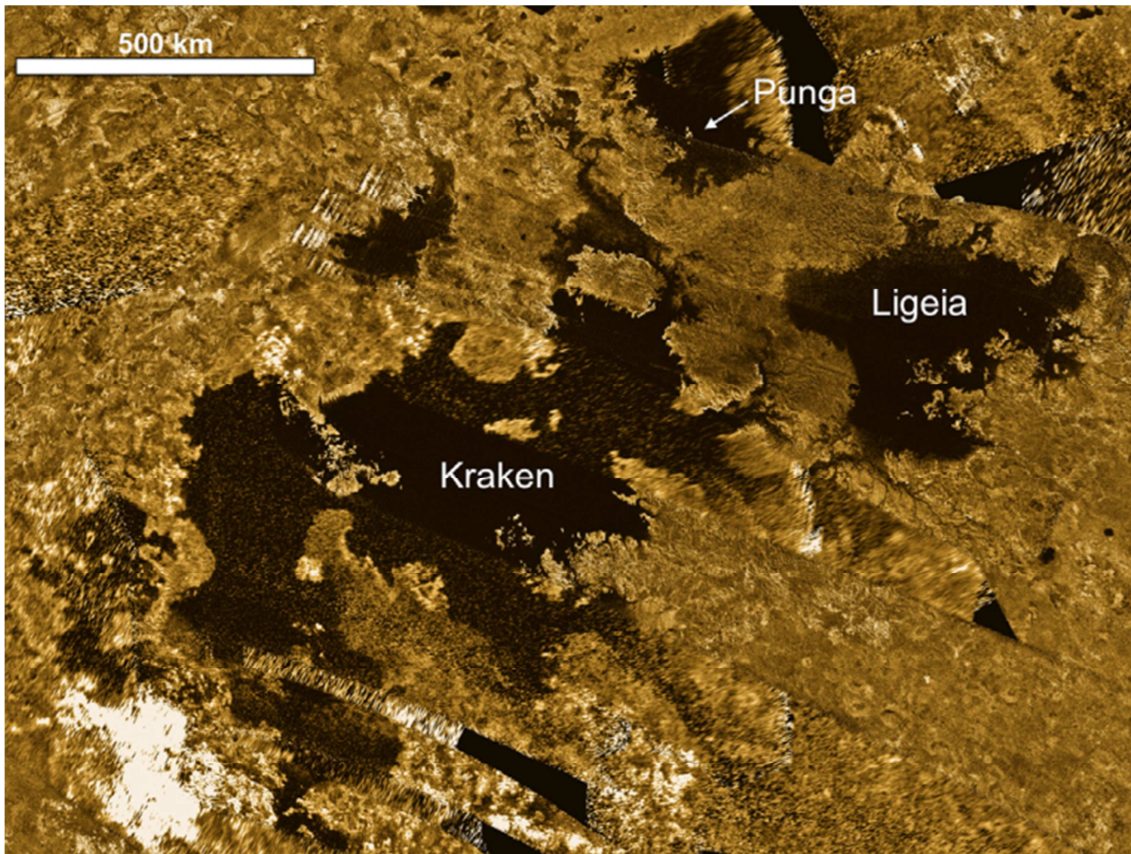
85

86 **Table 5.** E<sup>2</sup>T spacecraft technical characteristics.

E <sup>2</sup> T Spacecraft main technical characteristics		Heritage
<b>Spacecraft Dimensions</b>	<ul style="list-style-type: none"> <li>Main S/C body: 2974mm × 2860mm × 2589mm with 4 Solar Array wings of an overall area of 160 m<sup>2</sup>.</li> <li>SEPS cylindrical section: 600mm radius × 970mm height with 3+1 QinetiQ T6-Ion Thruster Engine of 7.5 kW each one.</li> </ul>	ExoMars BepiColombo
<b>Overall Launch mass</b>	<ul style="list-style-type: none"> <li>4056 kg (including 58 kg of science payload), dry mass 1876 kg</li> </ul>	
<b>Propulsion Architecture</b>	<p>The E<sup>2</sup>T S/C propulsion architecture is based on the integration of three different propulsion systems:</p> <ul style="list-style-type: none"> <li>Solar Electrical Propulsion System (SEPS) based on 3+1 QinetiQ T6 gridded Ion-Thruster engines (1 for redundancy)</li> <li>Main Bi-propellant propulsion system for S/C manoeuvres purposes</li> <li>Hydrazine Mono-propellant propulsion system of 16 RCS Thruster (8+8 in hot redundancy) for Attitude and Orbital Control System (AOCS) purposes.</li> </ul>	ExoMars BepiColombo
<b>Power Architecture</b>	<p>The E<sup>2</sup>T Electrical Propulsion System (EPS) architecture proposed is based on:</p> <ul style="list-style-type: none"> <li>4 Solar Array Wings able to sustain an End of Life (EOL) power demand of 620 W (including margins) with a reference solar constant of 15 W/m<sup>2</sup> at 9.14 AU, with a Sun-Aspect-Angle of 0°.</li> <li>One 31 kg Li-Ion battery of 3691 Wh total capacity and able to sustain a peak power load of demand of 700 W during the forecast eclipses.</li> <li>One secondary battery installed on SEPS module for 100 V High-Voltage Sun-regulated power bus stability purposes.</li> </ul>	JUICE Rosetta BepiColombo
<b>Baseline payload</b>	<ul style="list-style-type: none"> <li>Ion and Neutral Mass Spectrometer (INMS)</li> <li>Enceladus Icy Jet Analyser (ENIJA)</li> <li>Titan Imaging and Geology, Enceladus Reconnaissance (TIGER) high-resolution infrared camera</li> </ul>	

87

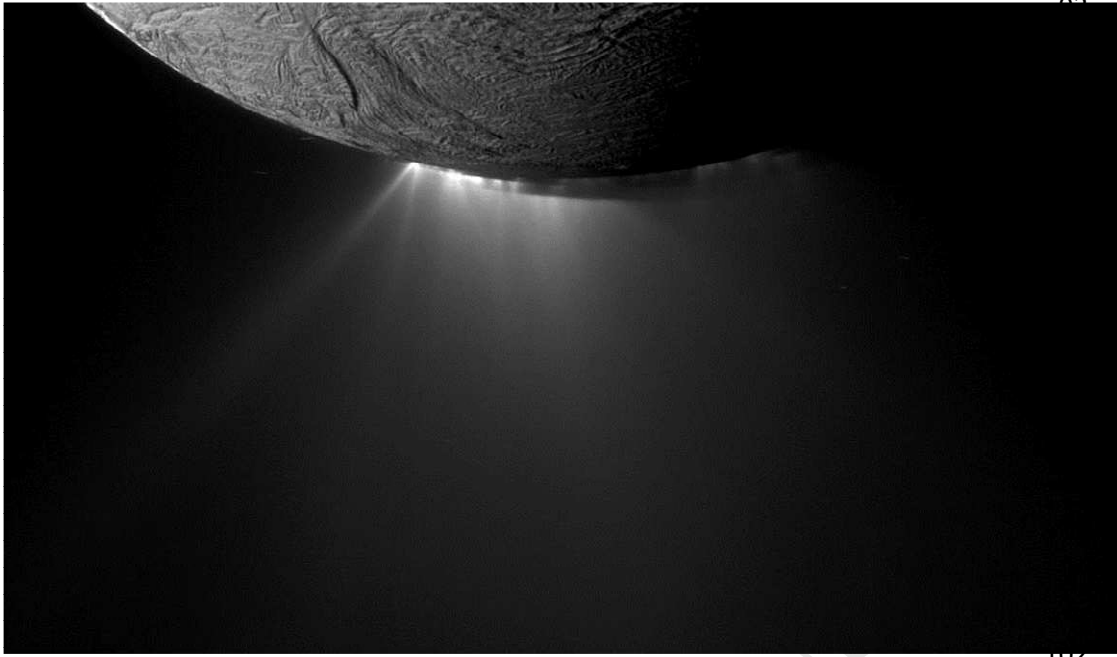
88



89

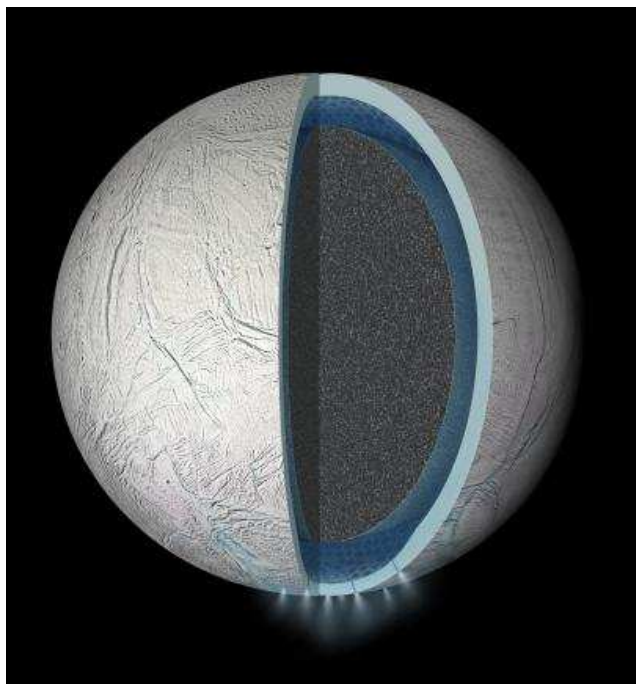
90 **Figure 1.** Cassini SAR mosaic images of the north polar region showing Kraken, Ligeia and Punga  
91 Maria (from Mitri et al., 2014a).

92



103 **Figure 2.** Plume emanating from multiple jets in Enceladus' south polar terrain  
104 (NASA/JPL/Space Science Institute).

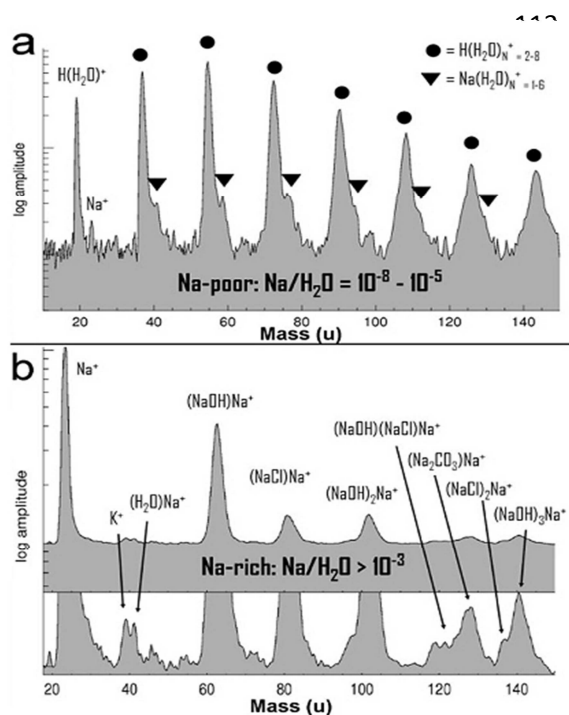
105



106

107 **Figure 3.** Enceladus' internal structure inferred from gravity, topography and libration  
108 measurement provided by Cassini mission. A global subsurface ocean is present under the  
109 outer ice shell. The ice shell is believed to be a few kilometers thin at the south polar region  
110 where the center of the geological activity is with the formation of the plume formed by  
111 multi-jets (NASA/JPL-Caltech).

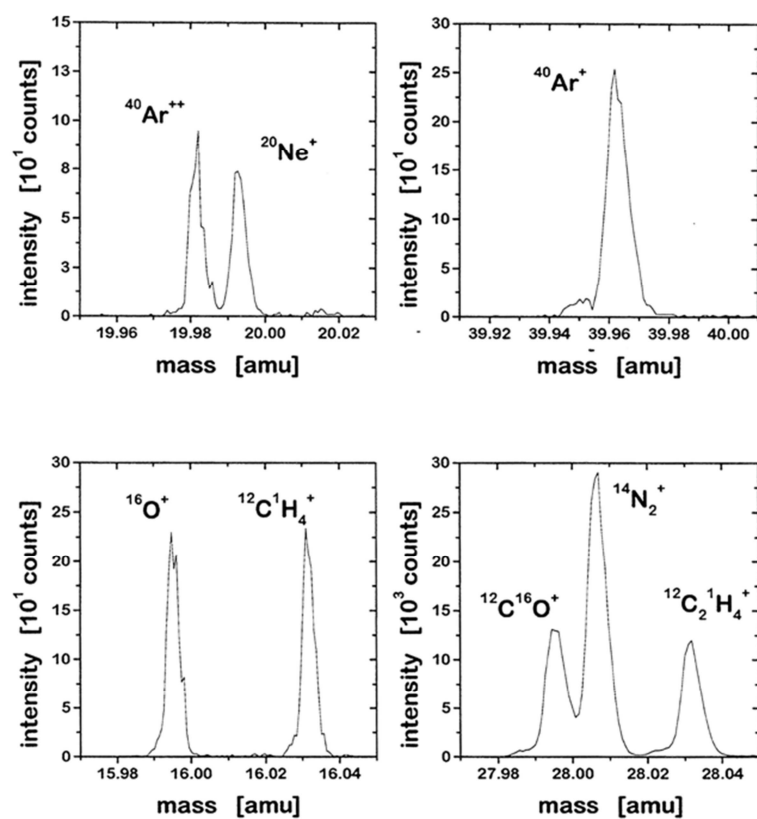
112



124 **Figure 4.** Composition of salt-poor (Type I and II) and salt-rich (Type III) particles in  
 125 Saturn's E-ring and Enceladus' plume as measured by Cassini CDA instrument (Postberg et  
 126 al., 2009).

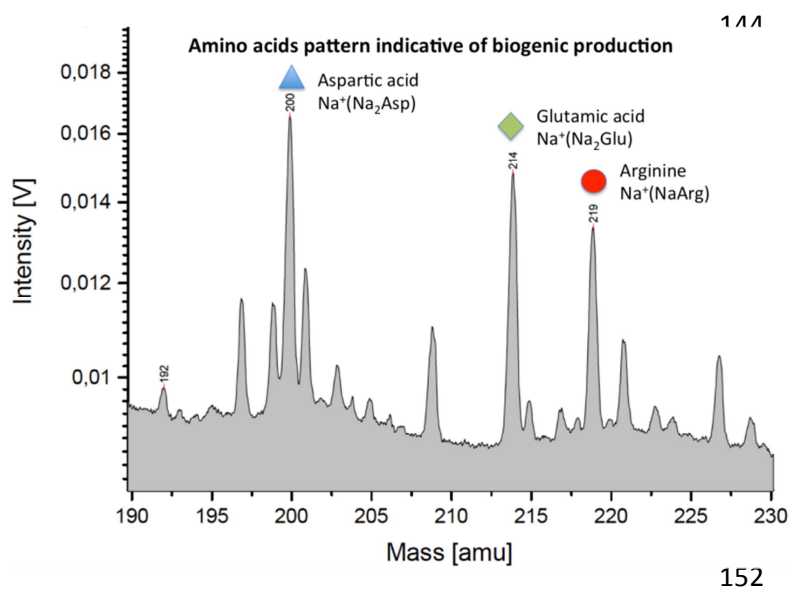
127





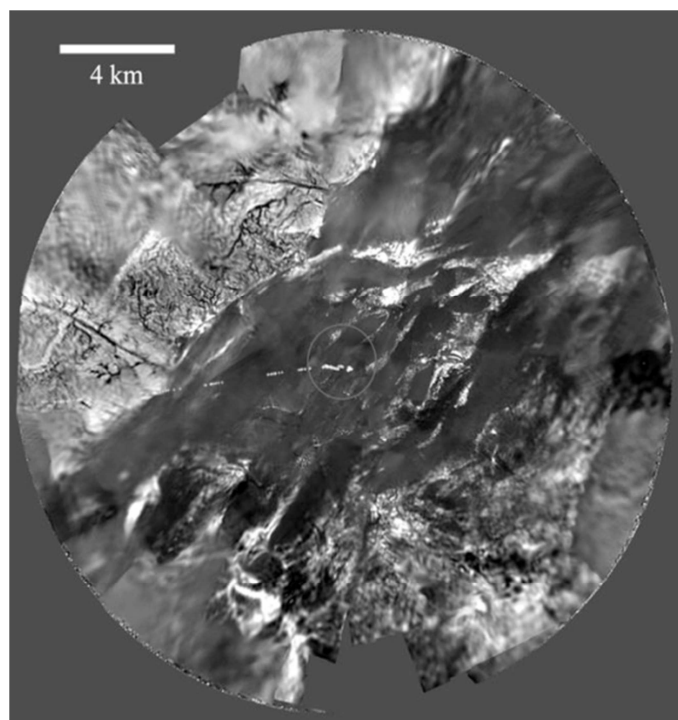
140 **Figure 5.** Separation of isobaric interference such as occur at 16, 20, 28, and 40 u/e for the  
141 indicated species is possible based on heritage of RTOF/ROSINA from the Rosetta mission  
142 (Scherer et al., 2006; Wurz et al., 2015).

143



153 **Figure 6.** Laser dispersion mass spectrum of aspartic acid (12 ppm), glutamic acid (12 ppm),  
154 and arginine (8 ppm) dissolved in a salt-water matrix simulating Enceladus' ocean  
155 composition. The complex amino acids are detectable in comparable quantities to glycine (15  
156 ppm, not shown), even though the spectrum has a mass resolution 3 times less than ENIJA's.  
157 S/N ratio of this laser dispersion spectrum is comparable to a much lower analysed  
158 concentration in ENIJA spectra ( $\leq 1$  ppm). Most un-annotated mass lines are due to salt-water  
159 cluster ions. By co-adding multiple ice grain spectra the S/N ratio can be further improved  
160 leading to an ENIJA detection limit of 10–100 ppb for most amino acids in ice grains formed  
161 from Enceladus' ocean water.

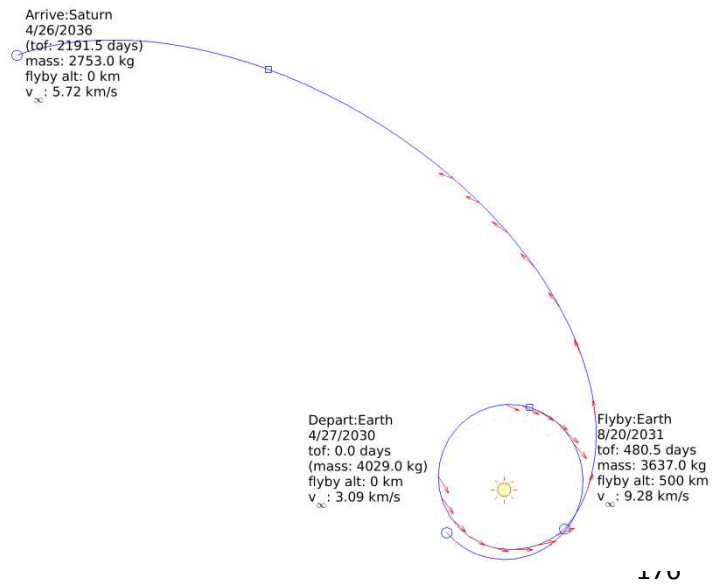
162



163

164 **Figure 7.** The surface of Titan imaged by DISR camera during the Huygens probe descend.  
165 TIGER has the capability to image Titan at Huygens DISR resolution  
166 (ESA/NASA/JPL/University of Arizona).

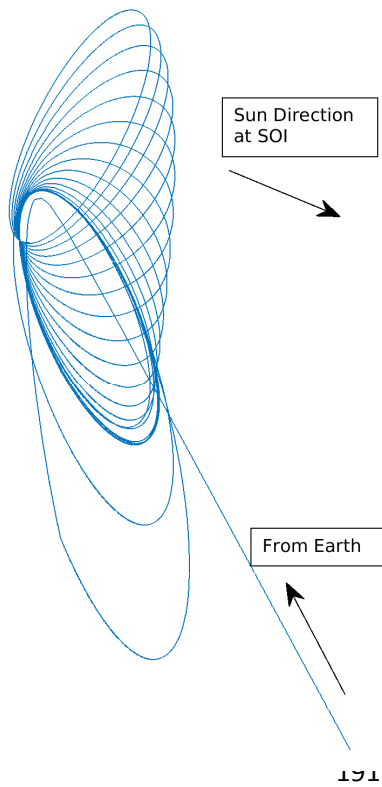
167



177 **Figure 8.** Interplanetary transfer to Saturn. Red arrows indicate electric propulsion thrust.

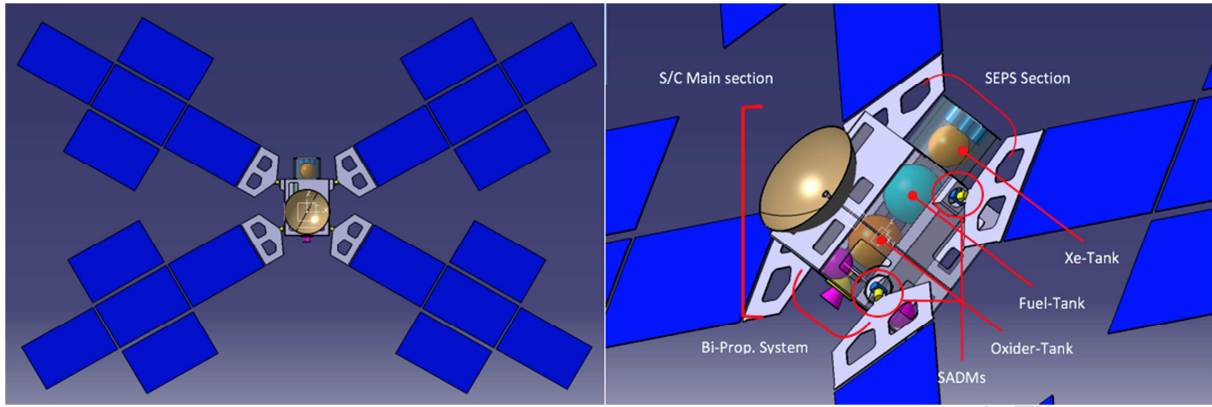
178

179



192 **Figure 9.** Sample tour with two period- and inclination-management Titan flybys followed  
193 by a science phase with 6 Enceladus flybys and 17 Titan flybys (Inertial representation).

194



195

196 **Figure 10.** E<sup>2</sup>T baseline proposed configuration of the spacecraft. Left panel shows an  
197 enlarged view of the S/C and right panel shows a close-up view of the spacecraft.

GOAL A: ORIGIN AND EVOLUTION OF VOLATILE-RICH OCEAN WORLDS, ENCELADUS AND TITAN						
Science Objectives	Scientific Questions	Measurement Description	Measurement Requirements			
			Payload	Parameter	Requirement	Performance
<b>A.1: Are Enceladus' volatile compounds primordial or have they been re-processed and if so, to what extent?</b>	Are major volatiles in the plume material primordial (as opposed to geochemical or biological) and, if so, how were they delivered?	Quantify the abundance of radiogenic and non-radiogenic noble gases (40/38/36 Ar, 4/3He, 20/22Ne, 128-136Xe) from mass spectra of plume vapour phases	INMS	Dynamic range Resolution Sensitivity	6/8 decades 5000 m/ $\Delta$ m 10 <sup>1</sup> #/cm <sup>3</sup>	6/10 decades 5000 m/ $\Delta$ m 10 <sup>0</sup> #/cm <sup>3</sup>
		Determine the extent of molecular complexity in the plume up to 1000 amu	INMS	Dynamic range Resolution Sensitivity	6/8 decades >300 m/ $\Delta$ m 10 <sup>1</sup> #/cm <sup>3</sup>	6/10 decades 5000 m/ $\Delta$ m 10 <sup>0</sup> #/cm <sup>3</sup>
		Measure isotopic ratios ( <sup>12</sup> C/ <sup>13</sup> C, D/H, <sup>14</sup> N/ <sup>15</sup> N, <sup>16</sup> O/ <sup>18</sup> O) in major species from mass spectra of plume vapour, including allowing the separation of species with isobaric interferences for example, <sup>12</sup> CH from <sup>13</sup> C	INMS	Dynamic range Resolution  Sensitivity	6/8 decades >2500-3000 m/ $\Delta$ m 10 <sup>3</sup> #/cm <sup>3</sup>	6/8 decades 5000 m/ $\Delta$ m  10 <sup>0</sup> #/cm <sup>3</sup>
		Measure isotopic ratio <sup>12</sup> C/ <sup>13</sup> C from mass spectra of condensed organics in icy grains	ENIJA	Dynamic range Mass range Resolution Sensitivity	3 decades 12–100m/z 100 m/ $\Delta$ m 1 ppm	6/8 decades 1–2000m/z 1000m/ $\Delta$ m 0.1 ppm
		Determine the abundance ratio between major C-, N-, O-, S-bearing compounds from mass spectra of plume vapour and solid phases, including allowing the separation of vapour-phase species with isobaric interferences for example, CO from N <sub>2</sub>	INMS  ENIJA	Dynamic range Resolution Sensitivity  Dynamic range Mass range Resolution Sensitivity	6/8 decades 3000 m/ $\Delta$ m 10 <sup>3</sup> #/cm <sup>3</sup>  5 decades 12–200 m/z 200 m/ $\Delta$ m 1 ppm	6/10 decades 5000 m/ $\Delta$ m 10 <sup>0</sup> #/cm <sup>3</sup>  6/8 decades 1–2000m/z 1000m/ $\Delta$ m 0.1 ppm

	Do Enceladus' volatile compounds originate from a unique reservoir and, if so, how is their distribution between solid and vapour phases affected by eruption processes?	Determine the compositional profile of major species through the plume (both volatile and non-volatile) from mass spectra of plume vapour and condensed phases in icy grains	INMS	Dynamic range Resolution Sensitivity	6/8 decades 300 m/ $\Delta$ m $10^3$ #/cm <sup>3</sup>	6/10 decades 5000 m/ $\Delta$ m $10^0$ #/cm <sup>3</sup>
			ENIJA	Dynamic range Mass range Resolution Sensitivity Spatial resolution	5 decades 7–500 m/z 500 m/ $\Delta$ m 1 ppm 1000 m	6/8 decades 1–2000m/z 1000m/ $\Delta$ m 0.1 ppm 100 m
<b>A.2: What is the history and extent of volatile exchange on Titan?</b>	How were Titan's volatiles delivered, and were they internally processed?	Quantify the abundance of noble gases in the atmosphere	INMS	Dynamic range Resolution  Sensitivity	6/8 decades 3000–5000 m/ $\Delta$ m $10^3$ #/cm <sup>3</sup>	6/10 decades 5000 m/ $\Delta$ m  $10^0$ #/cm <sup>3</sup>
		Measure and compare isotopic ratios: <sup>12</sup> C/ <sup>13</sup> C and D/H in the atmospheric main constituents	INMS	Dynamic range Resolution Sensitivity	6 decades 3000 m/ $\Delta$ m $10^5$ #/cm <sup>3</sup>	6 decades 5000 m/ $\Delta$ m $10^0$ #/cm <sup>3</sup>
	What is the age of Titan's methane cycle, and is there evidence for renewal from internal outgassing?	Measure and compare isotopic ratios: ( <sup>14</sup> N/ <sup>15</sup> N; <sup>12</sup> C/ <sup>13</sup> C; D/H; <sup>16</sup> O/ <sup>18</sup> O) in the upper atmosphere	INMS	Dynamic range Resolution Sensitivity	6/8 decades 3000 m/ $\Delta$ m $10^3$ #/cm <sup>3</sup>	6/10 decades 5000 m/ $\Delta$ m $10^0$ #/cm <sup>3</sup>
		Constrain the genesis of candidate cryovolcanoes and cryovolcanic flows	TIGER	Coverage  Scale Wavelength DTM vertical resol.	Sotra, Tui, & Hotei 50 m/pixel 3 colours 20 m	Sotra, Tui, & Hotei 30–50 m/pixel 3 colours 15–20 m
	How does Titan's surface reflect climate change?	Determine whether seas have existed in the tropics and/or south polar region	TIGER	Coverage  Scale Wavelength DTM vertical resol.	Regions within Hotei, Tui, Xanadu & the putative south-polar basins 100m/pix 3 colour N/A	Regions within Hotei, Tui, Xanadu & the putative south-polar basins 100m/pix 3 colour N/A
		Investigate fine-scale dune patterns and how they reorient or breakup	TIGER	Coverage Scale Wavelength DTM vertical resol.	4 dune regions 50m/pix 3 colour N/A	4 dune regions 30–50m/pix 3 colour N/A



<b>A.3: How has Titan's organic-rich surface evolved?</b>	How have liquid organics modified Titan's surface?	Investigate the morphology of river networks and channels	TIGER	Coverage Scale Wavelength DTM vertical resol.	3 drainages 30m/pix 3 colour 15 m	3 drainages 25–30m/pix 3 colour 10–15 m
		Determine whether the labyrinth terrains and sharp edged depressions are formed by dissolution	TIGER	Coverage Scale Wavelength DTM vertical resol.	2 regions 100m/pix 3 colour 40 m	2 regions 50–100m/pix 3 colour 20–40 m
	To what degree are sediments produced and transported by fluvial and eolian processes?	Investigate the margins of the dune fields to identify sources and sinks of sand	TIGER	Coverage Scale Wavelength DTM vertical resol.	4 dune regions 50m/pix 3 colour N/A	4 dune regions 30–50m/pix 3 colour N/A
		Determine the primary erosion processes that degrade impact crater rims	TIGER	Coverage Scale Wavelength DTM vertical resol.	4 impacts 100m/pix 3 colour N/A	4 impacts 50–100m/pix 3 colour N/A
		Investigate the fine-scale geologic processes that modify the plains	TIGER	Coverage Scale Wavelength DTM vertical resol.	3 regions 50m/pix 3 colour N/A	3 regions 30–50m/pix 3 colour N/A
	How do the mechanical and chemical properties (i.e., composition) vary between the observed geologic units on Titan?	Determine how fluvial erosion varies among geologic units	TIGER	Coverage Scale Wavelength DTM vertical resol.	5 regions 50m/pix 3 colour N/A	5 regions 30–50m/pix 3 colour N/A
		Constrain the maximum slopes and topography supported by different geologic units	TIGER	Coverage Scale Wavelength DTM vertical resol.	5 regions 100m/pix 3 colour 40m	5 regions 50–100m/pix 3 colour 20–40m
		Investigate the morphology, topography, and spectral relationships across unit boundaries	TIGER	Coverage Scale Wavelength DTM vertical resol.	5 boundaries 100m/pix 3 colour 40m	5 boundaries 50–100m/pix 3 colour 20–40m

GOAL B: HABITABILITY AND POTENTIAL FOR LIFE IN OCEAN WORLDS, ENCELADUS AND TITAN						
Science Objectives	Scientific Questions	Measurement Description	Instrument	Measurement Requirements		
				Parameter	Requirement	Performance
<b>B.1: Is Enceladus' aqueous interior an environment favourable to the emergence of life?</b>	What is the nature of hydrothermal activity on Enceladus and how does it connect with the plume activity?	Detect and inventory reduced and oxidized species in the plume material (e.g., NH <sub>3</sub> /N <sub>2</sub> ratio, H <sub>2</sub> abundance, reduced versus oxidized organic species)	INMS	Dynamic range Resolution Sensitivity	6/8 decades 3000m/Δm 10 <sup>3</sup> #/cm <sup>3</sup>	6/10 decades 5000m/Δm 10 <sup>0</sup> #/cm <sup>3</sup>
			ENIJA	Dynamic range Mass range Resolution Sensitivity	4 decades 7–200 m/z 200 m/Δm 1 ppm	6/8 decades 1–2000m/z 1000m/Δm 0.1 ppm
		Characterize composition and abundance of salts and other minerals as messengers of rock/water interaction from mass spectra of icy grains	ENIJA	Dynamic range Mass range Resolution Sensitivity	6 decades 7–200 m/z 200 m/Δm 1 ppm	6/8 decades 1–2000m/z 1000m/Δm 0.1 ppm
		Determine spatial variations in plume composition (vapour and icy grains) and correlate with source activity	ENIJA	Dynamic range Mass resolution Resolution Sensitivity Spatial Resolution	4 decades 7–500 m/z 500 m/Δm 1 ppm 1000 m	6/8 decades 1–2000m/z 1000m/Δm 0.1 ppm 100 m
			TIGER	Coverage  Scale Wavelength DTM vertical res.	2 cross-stripe tracks  5m/pix 5 & 5.3 μm N/A	2 cross-stripe tracks  2.5–5m/pix 5 & 5.3 μm N/A
		Determine how much energy the jets dissipate	TIGER	Coverage  Scale Wavelength DTM vertical res.	2 night-time cross-stripe tracks  5m/pix 5 & 5.3 μm N/A	2 cross-stripe tracks  2.5–5m/pix 5 & 5.3 μm N/A

	Is there evidence that biotic/prebiotic processes are operating in Enceladus' interior?	Compare mass distribution of organic molecules to that expected from abiotic synthesis (e.g., Poisson versus non-Poisson) in the mass distribution of organic molecules	INMS	Dynamic range Resolution Sensitivity	6/8 decades 3000m/Δm 10 <sup>3</sup> #/cm <sup>3</sup>	6/10 decades 5000m/Δm 10 <sup>0</sup> #/cm <sup>3</sup>
			ENIJA	Dynamic range Mass range Resolution Sensitivity	6 decades 26-1000 m/z 500 m/Δm 1 ppm	6/8 decades 1-2000m/z 1000m/Δm 0.1 ppm
		Search for abnormal isotopic ratio in organics in plume vapour, including allowing the separation of species with isobaric interferences for example, <sup>12</sup> CH from <sup>13</sup> C	INMS	Dynamic range Resolution Sensitivity	6/8 decades 2500-3000 m/Δm 10 <sup>3</sup> #/cm <sup>3</sup>	6/10 decades 5000 m/Δm 10 <sup>0</sup> #/cm <sup>3</sup>
		Search for amino acids and abnormal <sup>12</sup> C/ <sup>13</sup> C ratio in organics that may have been captured in the ice matrix of solid plume material	ENIJA	Dynamic range Mass range Resolution Sensitivity	5 decades 12-500m/z 500 m/Δm 1 ppm	6/8 decades 1-2000m/z 1000m/Δm 0.1 ppm
<b>B.2: To what level of complexity has prebiotic chemistry evolved in the Titan system?</b>	What chemical processes control the formation and evolution of complex organics in Titan's atmosphere?	Measure the elemental chemistry of low mass organic molecules in Titan's atmosphere	INMS	Dynamic range Resolution Sensitivity	6/8 decades 3000m/Δm 10 <sup>1</sup> #/cm <sup>3</sup>	6/10 decades 5000m/Δm 10 <sup>0</sup> #/cm <sup>3</sup>
		Measure organic macromolecules and ioni species (cations and anions) in order to monitor chemical coupling processes between ions and neutral species	INMS	Dynamic range Resolution Sensitivity	6/8 decades 3000m/Δm 10 <sup>1</sup> #/cm <sup>3</sup>	6/10 decades 5000m/Δm 10 <sup>0</sup> #/cm <sup>3</sup>
		Characterize the structure of haze layers, along with their spatial and temporal variations	TIGER	Coverage  Scale	10 temporally spaced full-disk images 1km/pix	10 temporally spaced full-disk images 500m-1km/pix

				Wavelength DTM vertical resol.	3 colours N/A	3 colours N/A
		Determine the cloud distribution and morphology, including estimates of their top altitudes and vertical extent	TIGER	Coverage  Scale Wavelength DTM vertical resol.	10 temporally spaced full-disk images 1km/pix 3 colours N/A	10 temporally spaced full-disk images 500m–1km/pix 3 colours N/A
	To what extent does Titan's organic-rich surface chemically communicate with its water-rich interior?	Investigate the morphology and compositional variability of candidate cryovolcanoes	TIGER	Coverage  Scale Wavelength DTM vertical resol.	Sotra, Tui & Hotei 50m/pix 3 colours 20m	Sotra, Tui & Hotei 30–50m/pix 3 colours 15–20m
		Investigate the morphology of Titan's mountains to look for evidence of compressional vs extensional tectonics	TIGER	Coverage Scale Wavelength DTM vertical resol.	3 mountains 100 m/pix 3 colours 40 m	3 mountains 50–100 m/pix 3 colours 20–40 m
		Investigate melt sheets and flows associated with impact craters	TIGER	Coverage  Scale Wavelength DTM vertical resol.	2 larger fresh craters 50 m/pix 3 colours N/A	2 larger fresh craters 30–50 m/pix 3 colours N/A
		Measure the abundance of radiogenically derived noble gases (e.g., $^{40}\text{Ar}$ , $^{21}\text{Ne}$ ) and helium	INMS	Dynamic range Resolution Sensitivity	6/8 decades 3000m/ $\Delta$ m $10^1 \text{ \#/cm}^3$	6/10 decades 5000m/ $\Delta$ m $10^0 \text{ \#/cm}^3$

**Highlights**

- We present a space mission concept, the Explorer of Enceladus and Titan (E<sup>2</sup>T), which is dedicated to investigating the evolution and habitability of these Saturnian satellites.
- E<sup>2</sup>T is proposed as a medium-class mission led by ESA in collaboration with NASA in response to ESA's M5 Cosmic Vision Call.
- E<sup>2</sup>T proposes a focused payload that would provide in-situ composition investigations and high-resolution imaging during multiple flybys of Enceladus and Titan using a solar-electric powered spacecraft in orbit around Saturn.